2024-04-10

Lithological controls on the timing of strath terrace staircase formation in a collisional mountain belt

Zondervan, J

10.1002/esp.5821
Earth Surface Processes and Landforms
Wiley

Lithological controls on the timing of strath terrace staircase formation in a collisional mountain belt

Jesse R. Zondervan[1,2*], Martin Stokes[1], Sarah J. Boulton[1], Matt W. Telfer[1], Anne E. Mather[1], Mhamed A. Belfoul[3]

[1] *School of Geography, Earth and Environmental Sciences, University of Plymouth, United Kingdom*

[2] *Now at: Department of Earth Sciences, University College London, United Kingdom*

[3] *Structural Geology and Thematic Mapping Laboratory, Ibn Zohr University, Morocco*

Correspondence to: Jesse R. Zondervan (j.zondervan@ucl.ac.uk)

Zondervan ORCID: 0000-0002-7862-3879
Stokes ORCID: 0000-0003-3788-4615 email: m.stokes@plymouth.ac.uk
Boulton ORCID: 0000-0002-8251-0025 email: sarah.boulton@plymouth.ac.uk
Telfer ORCID: 0000-0002-8562-7720 email: matt.telfer@plymouth.ac.uk
Mather ORCID: 0000-0001-6634-8681 email: a.mather@plymouth.ac.uk
Belfoul ORCID: 0000-0002-8268-4893 email: m.belfoul@uiz.ac.ma

Data Availability Statement

Terrace and modern river grain size, clast lithology and elevation data, in addition to DEM derived river profile and terrace elevations, and Schmidt Hammer rebound values are available as supplementary online information.

Funding

J.R.Z. acknowledges the BSG Postgraduate Research Grant, IAS Postgraduate Grant, and the QRA New Research workers Award which supplemented J.R.Z.'s University of Plymouth PhD scholarship. The authors also acknowledge funding in kind from the German Aerospace Center (DLR) in the form of the TanDEM-X data.

Acknowledgements

The authors thank Nawfal Taleb and Madeleine Hann for their assistance in the field. We thank Philip Prince and an anonymous reviewer for their constructive comments which helped us improve the paper's quality. We thank Mitch D'Arcy and Stuart Lane for their editorial guidance.

Author contributions

Conceptualization: JRZ; funding acquisition: JRZ, MS, AEM; methodology (including methodological development): JRZ, MS, SJB, MWT, AEM; investigation (e.g. data collection): JRZ, MS, AEM, SJB, MAB; supervision: MS, SJB, MWT, AEM; writing – initial draft: JRZ, MS; writing – reviewing and editing: JRZ, MS, SJB, MWT.

Conflict of Interest

The authors declare that they have no known competing financial interests or personal relationships that could have appeared to influence the work reported in this paper.

Lithological controls on the timing of strath terrace staircase formation in a collisional mountain belt

Abstract

In mountain belts, strath terrace staircases serve as markers for deriving river incision rates and erosional patterns. Distinguishing between terrace patterns influenced by external perturbations like changes in climate and tectonics, and those driven by internal dynamics including feedbacks between topography, erosion and sediment transport, remains challenging. We demonstrate that in a collisional mountain belt, lithology can act as a first-order control on the spatial and temporal scales of strath terrace formation. Here we investigate the role of lithology in modulating internal dynamics and the formation of strath terraces in the Mgoun River catchment of the High Atlas in Morocco, a region characterized by constant low-rate rock uplift, a cyclical cool-warm / arid-humid Quaternary climate history, and contrasting bedrock lithologies. By collecting: 1) modern river and terrace clast data; 2) bedrock strath and strath-top sediment elevations of four terrace levels; 3) terrace sedimentology, and 4) integration with published terrace chronology; we found a dominance of local sediment input from hillslopes, mostly from recycled bedrock conglomerates. Additionally, we found valley width, controlled by the stratigraphic and structural configuration of lithological erodibility, significantly impacts sediment connectivity. The isolation between valleys with varying widths results in varied timescales of river channel response to hillslope coupling, with hillslope-derived stochastic sediment gravity flows preserved in fluvial terraces in some river reaches and not in others. Furthermore, asynchronous terrace formation and abandonment ages result from the low longitudinal river connectivity between multiple valleys formed in erodible rock separated by gorges in high strength rock. These gorges limit knickpoint migration rates, inhibiting the ability of terraces formed in one valley to spread through the catchment. These findings can inform future research distinguishing between autogenic and external signals in erosional landscapes and help carefully derive river incision rates and climate insights from terraces.

Keywords: Strath terraces, Lithology, Internal dynamics, Erosional landscapes, High Atlas.

1 Introduction

Strath terrace staircases (or flights of strath terraces) in mountain belts are sequences of abandoned riverbeds cut into bedrock by river erosion (Leopold et al., 1964; Starkel, 2003), and are often used to derive long-term incision rates (e.g., Lavé and Avouac, 2000; Fuller et al., 2009; Burbank and Anderson, 2011; Pazzaglia, 2013; Schanz et al., 2018; Zondervan et al., 2022). Despite the considerable body of research on climatic or tectonic strath terrace formation in mountains (e.g. Seidl and Dietrich, 1992; Hancock and Anderson, 2002; Bridgland and Westaway et al., 2008, 2014; Finnegan, 2013; Cordier et al., 2017), their formation can also be affected by complex interactions between topography, erosion, and sediment transport (internal dynamics; Finnegan and Dietrich, 2011; Scheingross et al., 2020) independent from external perturbations such as climate or tectonics, making it challenging to disentangle signals in the patterns of these terrace staircases (Finnegan and Balco, 2013; Scheingross et al., 2020). A critical yet often overlooked factor in the formation of strath terraces in mountain belts is bedrock lithology (Montgomery, 2004), which can substantially influence river erosion, valley morphology and sediment supply (Sklar and Dietrich, 2001; Whipple et al., 2013), and hence the timescale at which internal dynamics affect strath terrace formation. Lithological control may be especially strong in the sedimentary stratigraphy of collisional mountain belts (e.g., Montgomery, 2004; Spotila & Prince, 2022), where contrasts in the cover sequence erodibility tend to be greater than in crystalline basement rocks or the heavily altered metamorphic bedrock of mountain belt cores, and where the tectonic

history of the orogen affects the spatial configuration of erodibility (e.g., Zondervan et al. 2020a).

Understanding the mechanisms that determine the timescales at which internal dynamics dominate strath terrace formation in mountains is in its early stages (Scheingross et al., 2020). In contrast to the more extensively studied external factors such as tectonic base-level changes (Seidl and Dietrich, 1992; Howard et al., 1994; Zaprowski et al., 2001; Jansen et al., 2011; Finnegan, 2013) and climate-induced sediment-water supply controls (Hancock and Anderson, 2002; Wegmann and Pazzaglia, 2002; Anthony and Granger, 2007; Rixhon et al., 2011; Bridgland and Westaway, 2014; Baynes et al., 2015; Beckers et al., 2015; DiBiase et al., 2015; Demoulin et al., 2017; Ortega-Becerril et al., 2018). Previous studies of terraces that addressed the timescale of internal dynamics have not exclusively focused on strath terrace staircases in mountain settings and have reported mixed results regarding the timescales of intrinsic versus climatic formation of river terraces. For example, in his review of European river systems Vandenberghe (1995) found a switch from large lowland terraced systems formed by internal dynamics to those formed by external perturbation at 10^3 to 10^4 year timescales. Meanhile, Bridgland and Westaway (2008, 2014) reported a dominance of climatically generated strath terraces at 10^5-year cyclicity in their global compilations of staircases. However, using an increase in the available chronological tools and data, studies have shown that direct relationships between interglacial-glacial climate, fluvial dynamics and strath terrace formation may not apply ubiquitously even at longer 10^5-year timescales, especially in mountain belts (Vandenberghe, 2005; Foster et al., 2017; Schanz et al., 2018; Zondervan et al., 2022). These discrepancies demonstrate a recognized need to understand the processes that affect the spatial and temporal signals of internal dynamics versus climatic forcing embedded in the spatial and temporal patterns of strath terraces and their staircases (Schanz et al., 2018; Scheingross et al., 2020).

In the sedimentary cover of collisional mountain belts, the configuration of hillslope and river channel lithologies may lead to patterns of terraces forming with a stronger imprint of intrinsic behaviour than in other settings. This is because sedimentary stratigraphy in collisional orogens is often characterised by high contrasts in bedrock erodibility, with folding, tilting and fault thrusting of stacks with variable widths in the thrust front and between wedge-top basins (Stokes and Mather, 2015; Mather et al., 2017; Mather and Stokes, 2018; Zondervan et al., 2020a). The resulting structural configuration and rock strength contrasts can affect both the morphology of strath terraces and the coupling of hillslope and river channel sediment transport (Stokes and Mather, 2015; Mather et al., 2017; Mather and Stokes, 2018). The configuration of hillslope and river bedrock stratigraphy can also modulate the propagation of sediment supply signals through river networks and influence knickpoint migration timescales (e.g., Whittaker et al., 2007; Whittaker and Boulton, 2012; Grimaud et al., 2016; Zondervan et al., 2020b; Wolpert and Forte, 2021), such as knickpoints propagating after initiation of local river incision and strath terrace formation (Baynes et al., 2018). Overall, these points suggest that lithology can play a first-order control on the spatial and temporal signals in strath terrace patterns, with asynchronous development driven by internal dynamics potentially being more common than previously considered, particularly within the sedimentary cover of collisional mountain belts. Studies show that internal dynamics modulating bedload sediment pulses can lead to stochasticity in river incision histories, leading to pitfalls in river incision rate derivations from strath terraces (Finnegan et al., 2014; Zondervan et al., 2022) or misinterpretations of climatic control on terrace formation (Korup, 2006; Zondervan et al., 2022).

Consequently, studies of river erosion, the delivery and transport of sediment, and strath formation predict a role for lithology in modulating internal dynamics in erosional landscapes. However, the challenge of constraining the timescales and interactions between sediment delivery, transport, and erosion during the strath terrace formation process remains a key frontier (Demoulin et al., 2017; Schanz et al., 2018). Addressing

this challenge requires an integrated dataset that characterizes the tectonic, climatic, lithological, and chronological contexts of a catchment. In this study, we focus on the Mgoun River catchment in the High Atlas of Morocco, where constant rock uplift, climatic history, lithological parameters, and chronological control on strath terraces and their sediments are available. Recognising that the strath terrace record is an integrator of river-hillslope sediment interactions and along-stream connectivity, we aim to constrain the temporal and spatial scales of internal dynamics of sediment supply, transport, and erosion, as well as their influence on strath formation. To achieve this, we collect data on the vertical and spatial locations of strath terraces, the sedimentology of their strath-top sediments, and quantitative clast size and lithological information from both terrace sediments and the contemporary river channel, integrating them with the chronology of strath surfaces and their deposits (Zondervan et al., 2022). Furthermore, we examine the impact of varying lithological and structural contexts of valleys hosting strath terraces on the spatiotemporal scales of these internal dynamics.

2 Setting

2.1 The High Atlas Mountains and the Mgoun River catchment

The High Atlas exhibits typical and distinctive characteristics of a collisional orogenic system, comprising a high-relief 'axial zone' bordered by thrust fronts, wedge-top and foreland basins (Chellai and Perriaux, 1996, El Harfi et al., 2001). The formation of the mountain range, 700 km in length and with peak elevations spanning 2 – 4 km, involved the inversion of a Mesozoic intracontinental rift system, followed by regional thrust faulting, folding, and lithospheric thinning (e.g., Gomez et al., 2000; Babault et al., 2008). Within the High Atlas, landscapes within the sedimentary cover exhibit the greatest spatial contrast in bedrock erodibility due to the distinct lithologies in this stratigraphic package, and their structural configuration is controlled by thin-skinned tectonics (Zondervan et al., 2020a).

The Mgoun River catchment incised into the sedimentary cover rocks of the High Atlas and serves as an example of how contrasts in bedrock erodibility can have a significant impact on landscape evolution. The Mgoun is a prominent regional river catchment with a watershed reaching up to 4,000 m above sea level. The drainage network has been shaped by Plio-Quaternary fluvial incision controlled by the exhumation of lithologies with variable hardness distributed spatially by the structural geology of the belt (Zondervan et al. 2020a; Zondervan et al. 2022). The river's path is mainly transverse and starts in the fold-thrust belt (FTB), after which it cuts across a series of parallel fold thrust stacks in the thin-skinned wedge-top basin (WTB) and thrust-front (TF) parts of the mountain belt (Figs. 1 & 2). This configuration means the river interacts with various lithological and structural elements of the orogenic system, directly influencing its valley morphology and sediment flux.

The catchment is characterised by a dryland hydrology and a little- or non-glaciated source of discharge and sediment throughout the Quaternary (Hughes et al., 2004; Zondervan et al., 2022), with low-rate base level lowering set by long-term rock uplift rates of 0.17–0.22 mm yr^{-1} during the last 15 Ma (Babault et al., 2008; Zondervan et al., 2022). Furthermore, the Mgoun River drains into the intracontinental Ouarzazate Basin, which has been unaffected by Quaternary eustatic sea-level or tectonic base-level changes (Boulton et al., 2014, Boulton et al., 2019; Zondervan et al., 2022). The development of strath terraces in the High Atlas region, including the Mgoun catchment, has primarily occurred during the Quaternary period (Arboleya et al., 2008; Stokes et al., 2017; Zondervan et al., 2022). Thus, Quaternary climate fluctuations are the main control on the evolution of the Mgoun strath terrace staircases, with the river's responses to these fluctuations modulated by internal dynamics affected by spatially variable rock erodibility. Whilst the trunk stream is perennial, most present-day geomorphic work is done by the activation of ephemeral tributaries during winter and spring storms that originate in the Mediterranean and rare storms derived from the tropics (Fink and Knippertz, 2003; Knippertz, 2003; Knippertz et al., 2003; Schulz et al.,

2008; Dłużewski et al., 2013; Stokes and Mather, 2015). Quaternary climatic history suggests eccentricity (~100 kyr) and, even more strongly, precessional (~26 kyr) cycles may impact geomorphic conditions in catchments on the southern side of the High Atlas (Tjallingii et al., 2008; Larrasoana et al., 2013; Dixit et al., 2020; Zondervan et al., 2021). However, detailed studies of strath terraces along the Mgoun River reveal weak correlation with these cycles (Zondervan et al., 2022).

2.2 Lithological composition and configuration along the Mgoun River

As the river exits the high relief (>1900 m elevation) fold-thrust belt (FTB) through a gorge in Jurassic limestones (Fig. 3a) it enters the open valley (~3.5 km wide) of an intermediate relief (1840 – 1960 m) wedge-top basin (WTB) dominated by Cretaceous red beds (Marls, see Table 1; Fig. 3b). Cretaceous red beds dipping shallowly to the south make up the valley floor, with valley walls of Jurassic folded and interbedded limestones and marls that grade into massive limestones. The river flows southeast obliquely across the wedge-top basin, flanked by low slopes on the eastern banks and steep slopes leading to a plateau of Pliocene conglomerates elevated ~100 m above the modern river on its western side (Fig.2). Lateral sediment fluxes into the river channel can come from tributaries and alluvial fans, with the potential for clasts recycled from terraces and Pliocene conglomerates (Figs. 2 & 3b).

In the downstream part of the wedge-top basin, the Mgoun cuts a deeply incised (> 200 m), ~ 2.5 km long and 20 to 50 m wide meandering gorge into structurally thickened Jurassic limestones (Fig. 3c). The Mgoun River emerges from the gorge into a high relief (1500 - 2000 m) thrust front zone (TF): a structurally complex ENE-WSW striking southward verging folded and oblique thrust-faulted sequence of Mesozoic and Cenozoic units (Fig. 3). The first valley contains a relatively confined floodplain (~150 to 375 m wide), running along strike through weak Eocene red beds, constrained by a valley wall of Mio-Pliocene conglomerates to the north and Eocene limestones to the south (Fig. 3d). Because the valley is narrow, the range of sediment inputs are more constrained, limited to fluxes from small tributary fans sourcing clasts from terraces and Mio-Pliocene conglomerates. The Mgoun River enters the Bou Tharar Valley (150 to 650 m wide; Fig. 3e) after flowing through a 200 m long gorge carved in Eocene limestone. The Bou Tharar Valley contains a confluence of this trunk stream with the second perennial trunk stream of the Mgoun catchment (Figs. 2 and 3f). The valley runs along-strike through weak Eocene red beds and is confined by high cliffs of Eocene limestone on either side (Fig. 3g). The narrow valley and lack of conglomerates constrains sediment sources to fluxes from upstream, direct hillslope supply and one or two tributaries sourcing from bedrock and terraces. The Mgoun River enters the Ait Saïd Valley after flowing through a 400 m long gorge carved in Eocene limestone (Fig. 3h). The Ait Saïd Valley is contained by more widely spaced Eocene limestone thrust stacks (~ 2 km apart) through which the river cuts an oblique transverse route (Fig. 3i). Mio-Pliocene conglomerates line the northern side of the valley, and the valley floor (~ 250 to 750 m wide) incises through weak Eocene red beds. Sediment sources to the river channel here include extensively gullied terraces and Mio-Pliocene deposits and tributary fans.

3 Methods

3.1 Strath terrace elevation, treads and the river profile

Strath terraces along the Mgoun River were mapped from the town of Aït Toumert in the WTB (Fig. 2) downstream to Aifar at the end of the TF (Fig. 2). Strath terraces were identified using standard morphological and geological criteria such as low-relief low-slope (<5°) surfaces (treads), presence of rounded and imbricated fluvial clasts and in most, but not all, sites an identifiable bedrock strath (Mather et al., 2017; Stokes et al., 2012). Where slope material covered the top of fluvial conglomerates this contact was identified using differences in sediment textures and fabrics (Mather et al., 2017).

Using topographic analysis of the 12 m per pixel TanDEM-X supplied by the German Aerospace Centre (https://tandemx-science.dlr.de/), surfaces with slopes of < 5° were used to map the terrace treads, which were subsequently targeted for field investigation (Fig. 2). For plotting along-stream treads, terrace-top heights above the river profile were extracted from the DEM at 12 m intervals along the inner valley terrace margins (closest to the modern river). Where possible, the height above the active channel of both the strath surface and the tread of the overlying fluvial sediments were recorded in the field using a Trupulse 360B laser range finder and Geo-X7 GPS. Terraces were defined using a letter and numbering system with T1 being the lowest and youngest strath terrace, and subsequent higher straths corresponding to T2 and T3 etc (Fig. 4). A combination of terrace strath and tread heights extracted from the DEM and measured in the field, together with the modern river long profile, was used to compare terrace positions along the length of the modern river (see Supplementary Information Fig. S2). Based on evaluation of available DEMs to extract hydrological networks in mountainous terrain (Boulton and Stokes, 2018), the ALOS world AW3D (Tadono et al., 2014) 30 m digital elevation model (DEM) was used to derive the river long profile and identify knickpoints.

3.2 Strath terrace sedimentology and approach to chronology

Prominent terraces with accessible and well-preserved sections from strath to fluvial top had previously been targeted for OSL sampling (Zondervan et al., 2022) and were described and logged using sediment facies analysis (Miall, 1978) enabling the interpretation of depositional environments (Supplementary Information Tables S1 & S2). OSL chronology allows dating of aggradation of the entire strath-top sediment stratigraphy, illuminating periods of gravel aggradation during occupation of the strath by the riverbed, as well as the eventual abandonment of the strath during incision and deposition of overbank fines (Zondervan et al. 2022). To track patterns of strath terrace formation, the dates of river occupation from bedload gravels were targeted at three sites along stream, from accessible terrace deposits within the age limit of OSL dating (Fig. 4). As a result, the degree of synchronicity of terrace formation between valleys through which the trunk stream of the Mgoun River flows can be determined. Furthermore, for each terrace and modern riverbed locality, we measured clast imbrication of 100 clasts over an area of 1 m^2 to constrain downstream palaeoflow direction.

The lithology of coarse sediment fractions in terraces and the modern channel is derived from bedrock sources in the FTB upstream of the study reach, notably Triassic red sandstone, Triassic igneous rocks, and Jurassic grey limestone, together with local sources of Eocene limestone and Pliocene and Mio-Pliocene conglomerates in the TF, which contain these lithologies (Tesón et al., 2010; Tesón and Teixell, 2008). To constrain sediment provenance and transport dynamics, we measured the grain-size distribution and lithologies of clasts in terraces and the modern river channel by Wolman point counting (Attal and Lavé, 2006; Whittaker et al., 2010; Whittaker et al., 2011; Wolman, 1954), recording clast lithology for each grain-size measurement (100 per count, Brozovic and Burbank, 2000; Dubille and Lavé, 2015; Quick et al., 2019). To average out the effects of individual flows in the terrace conglomerate deposit cross-sections, we collected grain-size from the full vertical extent (usually 2 to 3 m). High-flow channel bars were selected for measurements in the modern channel, as these are assumed to represent the deposition reflected in the terrace deposits. For each count, the long axes (the *a* axis, c.f. Watkins et al. 2020) of 100 clasts measuring > 1 mm in diameter were recorded over a 1 m^2 Wolman point count to estimate the median grain-size value, D_{50}, and the 84th and 96th percentiles, the D_{84} and D_{96} respectively. Clasts were selected randomly (c.f. Duller et al., 2010; Whittaker et al., 2011). Estimated sampling error for grain-size measurements are ±15%, similar to those in Whittaker et al. (2011) and Dingle et al. (2016). Downstream fining rates along the length of the surveyed river were calculated using Sternberg's exponential function:

$$D_x = D_0 e^{-ax} \quad \text{Eq. 1}$$

Where D_0 is the predicted input or initial characteristic grain-size, a is the downstream fining exponent and x is the distance downstream (Sternberg, 1875). The selective transport of particles and their abrasion control downstream fining rates in fluvial systems (Attal and Lavé, 2006; Duller et al., 2010; Fedele and Paola, 2007; Ferguson et al., 1996; Paola et al., 1992; Rice and Church, 2001). On the other hand, lateral input and recycling of sediment within valleys can disturb such fining trends (Dingle et al., 2016; Quick et al., 2019; Rice and Church, 2001).

3.3 Rock strength measurements

To quantify the rock strength of lithostratigraphic units affecting valley morphology and terrace occurrence, we use published geological maps (Fig. 2) and *in situ* measurements of compressive strength. Typically, ten to twenty Schmidt hammer (N-type) measurements (Goudie, 2006) were taken at each location, totalling 434 readings throughout the study area with up to 90 readings per geological unit (Table 3.1). The standard deviation of Schmidt hammer measurements reflects the variation of rock strengths within the lithological units (Table 1). Mean and standard deviation of Schmidt hammer rebound values (SHV) are then converted to estimates of uniaxial compressive strength (UCS) using the conversion which was derived by Katz et al. (2000) ($UCS = 2.21e^{(0.07\,SHV)}$) for a range of carbonates, sandstone and other rocks with a range of UCS values similar to those found in the study area.

4 Results

In the configuration of thrust stacks and valleys (Fig. 2), combined with rock strength measures (Table 1), we observe a consistent relationship between the spatial distribution of rock strength and valley morphology through the wedge-top basin and thrust front. The width between the (re-)occurrence of very erodible red beds (uniaxial compressive strength ~ 10 – 14 MPa) and moderately resistant to resistant limestones (39 – 90 MPa) align with the widths of valleys, and in turn the size of landforms in the hillslope-to-channel transition (e.g., tributaries, tributary fans, alluvial fans: section 2.2).

In addition to valley width, the structural configuration of lithological strength directly affects strath terrace positions in the wedge-top basin and thrust front. Strath terraces occur in three river reaches flowing through open valleys formed in weak Eocene red continental marls in the thrust front and Cretaceous red marls in the wedge-top basin (10 to 14 MPa; Figs. 2-4 and Table 1), separated by gorges formed in strong limestone bedrock (39 to 99 MPa; Fig. 2 and Table 1). The terrace levels and patterns vary between reaches along the 30 km river channel surveyed (Figs. 2 & 4, see section 4.1), so we define terrace stratigraphy in each reach independently.

The chronology of riverbed occupation and gravel aggradation also shows how the three reaches, which are separated by gorges in strong rock, have different stratigraphic relationships. This is especially clear in the contrast between the wedge-top basin and thrust front. Terrace T2 in the wedge-top basin is occupied over the period 128 – 59 ka, which overlaps with two terrace levels in the thrust front where occupation of T2 over 170 – 108 ka and T1 over 74 – 57 ka is separated by a period of incision (Fig. 4; Zondervan et al., 2022). However, to fully appreciate the chronological and spatial patterns of terrace formation, we need to integrate the data from strath treads and the modern river long profile with terrace chronology of staircases.

4.1 Strath terrace patterns: staircases, treads and chronology

Straths in staircases have different elevations and strath deposit thicknesses in the three reaches from the wedge-top basin upstream to the two reaches in the thrust front downstream. In the upstream Ait Toumert reach in the WTB, a staircase of four terrace levels, reaching up to ~60 m above the modern river plain, exhibits constant 10-15 m vertical steps and spans over 10 km (Fig. 4a). In the midstream Bou Tharar reach, three

strath levels are preserved, including the highest documented strath terrace in the study area at approximately 100 m above the modern river plain (T3, Fig. 4b). T2 has a bedrock strath 20 m above the floodplain and is covered in 10 m of fluvial deposits. The strath surface of T1 is at a similar elevation as T2, with the difference being that it is stripped of sediment. Further downstream, there are three terrace levels in the Ait Saïd reach (Fig. 4c). T1 is found directly next to the modern river plain throughout the valley, with a strath height of about 10 m and a 3 to 5 m thick deposit. T2 and T3 are preserved as extensive surfaces incised by gullies, with bedrock straths at elevations of 40 and 60 m above the modern river plain, respectively, and up to 10 m thick deposits.

The connection between the different staircases and their terrace-level stratigraphy (relative elevations and ages of terraces) over the three reaches can be further understood in the context of strath treads and the profile of river channel elevation along upstream distance (Fig. 5). In the downstream Ait Said reach and midstream Bou Tharar reach, terrace levels show variation in elevation and number over a 13 km along-stream distance (Figs. 5 & S2). For example, in the downstream Ait Said reach, the strath of T2 lies 30 m above the strath of T1, which itself is 10 m above the modern river plain. While in the midstream Bou Tharar reach, these straths do not differ significantly in elevation, where a T2 strath level at 20 m above the modern river plain covered by 10 m of fluvial deposits has been eroded to the strath level, approximately 19 m above the modern river plain, to form T1 (Fig. 5). A longitudinal profile of the river channel and the terrace treads reveals that these differences in terrace elevations are due to the upstream propagation of waves of incision through knickpoints (Figs. 5 & S2). Two knickpoints can be seen in the modern river profile (Figs. 4 & 5). These two knickpoints coincide with gorges through resistant limestone bedrock with uniaxial compressive strengths of 39 to 90 MPa (Table 1), but not all gorges in resistant limestone bedrock coincide with knickpoints. T1 and T2 terrace treads abut against a knickpoint in the thrust front, upstream of which no strath incision has occurred after the deposition of the thick T2 sediment. The merging of erosional bedrock treads of T1 and T2 just downstream of this knickpoint constrains a previous position of the knickpoint before T1 incision (Fig. 5). In the TF, the top OSL dates constraining the age of abandonment (Zondervan et al., 2022) show a decreasing age of T2 abandonment from the downstream Ait Said reach (105 ka) to the mid-stream Bou Tharar reach (<84 ka) 10 km upstream (Fig. 5).

4.2 Facies: process of sediment flux into river channels (lateral)

The Mgoun catchment terrace sedimentology features seven genetic lithofacies (Supplementary Information Table S1) that make up three architectural elements (Supplementary Information Table S2). The lithofacies range from poorly-sorted, clast-supported conglomerates indicating debris flow or hyperconcentrated flow (see also Stokes and Mather (2015) and Mather and Stokes (2018) for modern analogues in the study region), to red to tan-coloured sand, silt, and mud with fine lamination, suggesting overbank, abandoned channel, or waning flood deposits. The architectural elements consist of stratified conglomerates representing braided fluvial channel gravel bars and bedforms, inversely graded and massive conglomerates indicative of sediment gravity flows in alluvial/tributary fans or slope colluvial systems, and sand-mudstone sheets corresponding to floodplain deposits. These elements exhibit varying thickness, geometry, and lateral extent, reflecting the diverse sediment-supply and river channel interaction along the Mgoun River.

We observe that terrace deposits vary longitudinally along the stream, with similarities in facies architectural elements in terraces within vertical staircases (Supplementary Information S2). Notable differences in facies exist between the upstream Ait Toumert reach in the WTB and the midstream and downstream reaches of Ait Said and Bou Tharar in the TF. In the upstream Ait Toumert reach, T2 terrace deposits consist of either gravel bedform or sediment gravity flow and floodplain facies, with deposits interpreted as gravel sheets and lag deposits, indicating shallow water braided fluvial processes (Fig. 6a). Additionally, a T2 tributary terrace and an alluvial fan terrace

preserve sediment gravity flows, which could be attributed to debris flow and/or hyperconcentrated flows. In contrast, the midstream Bou Tharar reach, T2 and T3 deposits show evidence of dominantly braided fluvial processes, with transverse bar migration on top of the strath surfaces and the preservation of sedimentary structures pointing to higher water depth to clast size ratios than in the upstream Ait Toumert reach (Fig. 6b). The lower bed-roughness derived from the well-sorted nature of the conglomerates that form the upstream source of bedload for the Bou Tharar reach, the confined nature of the valley, and the confluence with a second perennial trunk stream in the valley, which increases discharge, may all contribute to the well-sorted braided fluvial processes with high water depth in this reach (Fig. 2).

In the downstream Ait Said reach, T2 deposits exhibit braided fluvial processes, with deposits interpreted as transverse bedform or channel fill to overbank or abandoned channel backswamp deposits (Fig. 6c). The overbank facies extend over a large area and are up to 2 m thick, suggesting a combination of abandonment and successive overbank flooding and later reoccupation, reflecting switching between aggradation and incision dominated environments.

4.3 Clast lithology and grain size trends: provenance and transport (longitudinal)

Clast lithological distribution systematically changes from reach to reach (Fig. 7a). Resistant fossiliferous limestone clasts enter the river channel and terraces at confluences with perennial tributaries draining the eastern side of the FTB. However, downstream of these confluences, none of the fossiliferous limestones are found in the river or terrace deposits. These transitions coincide with the presence of pre-Quaternary conglomerates in the hillslopes. Furthermore, grain size trends vary between reaches: weak trends in the upstream Ait Toumert reach; stronger trends in the midstream Bou Tharar, and non-existent trends in the downstream Ait Said reach (Fig. 7b).

In the upstream Ait Toumert reach, we observe a lack of fining in the median grain-size (D_{50}), with insignificant trends exhibiting a low fining exponent (Eq. 7b) of 0.001 and an r^2 of 0.001. Whilst still not statistically significant, the fining exponents and r^2 values increase for the D_{84} and D_{96}, with fining exponents of 0.009 and 0.018 and r^2 values of 0.050 and 0.133, respectively (Fig. 7b). The lateral input from tributaries and alluvial fans is reflected in the clast lithologies of the terraces, with every T2 surveyed displaying a different distribution and combination of lithologies (Fig. 7a).

For example, of fossiliferous Jurassic limestone is present in the downstream T2 deposits along the perennial tributary channel and near its confluence with the Ait Toumert reach (Supplementary Information Fig. S5c,e), and quartzites are present in one T2 deposit along the perennial tributary (Supplementary Information Fig. S5e). Consequently, the lack of a fining trend in the median grain size (Fig. 7b) is attributed to the lateral input and reworking of terrace, alluvial-fan, and tributary deposits as well as the Pliocene conglomerate units present in the valley (Figs. 2 & 7).

The midstream Bou Tharar reach has the highest relief and most confined valley (150 to 650 m wide; Fig. 2) along the studied length of the Mgoun River, and it is the only reach along which there is no source for recycling of pre-Quaternary hillslope conglomerates (Fig. 2). A major perennial trunk stream sourcing gravels from Pliocene conglomerates in a neighbouring wedge-top basin joins the surveyed trunk stream at a confluence in this reach, which is the likely source of the clasts of fossiliferous Jurassic limestone and Triassic pebble conglomerate not seen elsewhere (Fig. 7a). The Bou Tharar reach exhibits the strongest fining trends within the study area, with a fining exponent and r^2 of 0.071 and 0.334, 0.019 and 0.054, 0.038 and 0.199 for the D_{50}, D_{84} and D_{96} respectively (Fig. 7b). Opposite to the upstream Ait Toumert reach in the WTB, where the strongest fining trend is in the D_{96}, the strongest r^2 and fining exponent in Bou Tharar is that of the D_{50}.

In the downstream Ait Said reach, the consistent clast lithological distribution between terrace levels and modern river deposits (Fig. 7a), and the lack of downstream fining (Fig. 7b), point to recycling of conglomerates from terraces and the Mio-Pliocene conglomerate units. Except for the locally derived Eocene *Gryphaea*-bearing limestone, the clast lithological distribution is very similar to that in the other reach with Mio-Pliocene hillslope conglomerates (Fig. 7a). The coarser grain sizes downstream where tributaries sourced from Mio-Pliocene conglomerate headwaters join the axial river plain (Figs. 7b and S9) reflect lateral input into the fluvial system.

5 Discussion

We will use the results presented so far to demonstrate how the interplay between lithology, its spatial distribution, sediment flux and river incision significantly contributes to the internal dynamics forming asynchronous terrace staircases in the Mgoun River catchment. This idea challenges the traditional understanding of terrace formation as direct expression of climatic or tectonic signals.

The framework for the resulting discussion sections rests on the flow of arguments that start with the idea that sediment flux in the river channel is dominated by local influx from hillslopes, tributaries and alluvial fans (section 5.1). We present evidence from sediment character data (section 4.3) for the importance of local sediment input and that recycling of pre-Quaternary conglomerates in the wedge-top basin and thrust front are a likely cause (section 5.1). In turn, the dominant role of local sediment input means local river channel sediment content over time depends on the connectivity of local sediment sources to the river channel. This connectivity is controlled by the width of valleys that affect the size and timescale of buffering landforms, such as small tributary fans and larger alluvial fans (section 5.2). The difference in lateral sediment connectivity between the valleys is supported by changes in the facies of sediments preserved in the river terraces (Section 4.2). Finally, the differences in lateral sediment connectivity lead to differences in local forcings on incision and aggradation over time. However, whether local incisional histories are a result depends on the erosional connectivity of the river, which is affected by the presence of hard rock gorges (section 5.3). The river long profile evolution recorded by river terrace treads (Section 4.1) and abandonment ages shed light on how lithology affects the degree of isolation of the river reaches. The resulting strath terrace staircase formation is highly dependent on local conditions in river reaches separated by gorges, with various timings that make direct interpretations of climatic or tectonic drivers challenging. Discussing how the lithological distribution of thrust-fronts and wedge-top basins of collisional mountain belts result in such irregular patterns of terrace formation helps us understand in which settings internal dynamics might be important drivers of strath terrace formation (Section 5.4).*5.1 A dominance of local sediment flux*

By influencing the degree of control that local hillslope sediment fluxes have on the river channel, hillslope and bedrock lithology controls the extent of isolation between valleys in their response to climatic fluctuations over time. We found that the ratio of longitudinal downstream sediment transport to lateral sediment flux, where lateral sediment flux originates from hillslopes and landforms such as alluvial fans (Mather et al., 2017), is controlled by lithology and structure. We observed the recycling of bedrock conglomerates, which is common in thin-skinned tectonic settings (Dingle et al., 2016; Quick et al., 2019), has caused the coarse-grained sediment in the river channel to reflect local provenance. In the wedge-top basin (WTB) and thrust front (TF), hillslopes contain Pliocene and Mio-Pliocene conglomerates re-exposed in thrust stacks (Fig. 8a) in all reaches except the midstream Bou Tharar reach in the TF (Figs. 2, 3, 7). Terrace and modern gravel bars typically have a large share of the strongest rock types found in the catchment (~ 30 – 80 % limestone), a narrow grain size distribution (D_{50} to D_{84} between 20 and 90 mm), and well-rounded pebbles, characteristic of conglomerate recycling (Quick et al., 2019). Notably, the similarity of clast lithological distributions in reaches with geographically and chronologically similar palaeoconglomerates suggests that

conglomerate recycling is likely the dominant source of clasts within each reach, overprinting any signature from upstream (Fig. 7). In addition to conglomerate recycling, increasing local hillslope influx of gravels, the combination of the resultant narrow grain-size distribution (D_{50} to D_{84} between 20 and 90 mm, see Fig. 7b) and well-sorted, well-rounded (Supplementary Information S2.1) pebbles in the river channels facilitates the observed imbrication. These factors may make the bedload harder to entrain (Komar and Li, 1986; Quick et al., 2019) and would increase the thresholds for fluvial incision. Consequently, as higher incision thresholds increase the likelihood of heavy-tailed erosional hiatuses (Ganti et al., 2016; Zondervan et al. 2022), the effect of conglomerate recycling on sediment character could contribute to the stochastic nature of terrace occupation and episodic incision observed in the Mgoun River (Zondervan et al. 2022).

The dominance of lateral over longitudinal sediment flux is also evident in grain-size trends. In contrast to longitudinally connected river systems, where steady decreases in grain-size along linear or exponential trends occur (Attal and Lavé, 2006; Duller et al., 2010; Fedele and Paola, 2007; Ferguson et al., 1996; Paola et al., 1992; Rice and Church, 2001), grain-size trends are interrupted from reach to reach. Even in the midstream Bou Tharar reach, with the strongest fining trends, fining rates are lower than in other field studies (Attal and Lavé, 2006; Duller et al., 2010; Fedele and Paola, 2007; Ferguson et al., 1996; Paola et al., 1992; Rice and Church, 2001). Thus, the coarse grain-size fraction of the Mgoun River in the WTB and TF are dominated by lateral sediment flux recycled from palaeoconglomerates (Fig. 8). Taken together, the observations from clast lithology and grain-size demonstrate that lithology influences the relative local contributions of downstream sediment flux and sediment flux from hillslopes.

In addition to a large flux from lateral valley sources, the low ratio of longitudinal to lateral sediment flux could be owing to low longitudinal transport connectivity. Unsaturated groundwater systems in porous sedimentary rocks and karstic aquifers diminish hydrologic flow through infiltration in the Mgoun River channel (Cappy, 2006; de Jong et al., 2008). In addition, geomorphic barriers to sediment flux, such as valley constrictions, sediment slugs, and over-widened channels, have been shown to contribute to low longitudinal connectivity in other studies (Fryirs, 2013; Fryirs et al., 2007).

5.2 Valley morphology controls the response-time of local sediment sources

The dominance of lateral sediment flux over longitudinal river transport, to which lithology contributes as discussed in Section 5.1, enhances the control of valley morphology on local river sediment transport and incision processes. Valley morphology in turn is also controlled by lithology and thrust stack structure. The valley width, set by thrust stack spacing, affects the spatial scale of distributive fluvial systems; such as alluvial or tributary fans, their temporal connectivity with the channel, and the timescale of stochastic sediment flux into the river channel (Fig. 8; Stokes and Mather, 2015; Mather et al., 2017; Mather and Stokes, 2018). Because lateral sediment flux is the primary source of coarse sediment bedload in the Mgoun river channel, landforms that connect hillslope sediment generation and delivery to the trunk river channel play a significant role in determining the river channel sediment content over time.

In the unconfined, approximately 3.5 km wide valley of the wedge-top basin, river terraces preserve inversely graded and massive conglomerate deposits, indicative of sediment gravity flows derived from tributaries and large distributary fans (Section 4.2; Supporting Information S2; Fig. S5). Mather et al. (2017) demonstrated that alluvial fans in the High Atlas had limited coupling with the trunk river during fan-building periods. In contrast, periods of river incision induced partial buffering by alluvial fans, which connect via an active channel incising into the deposit. Consequently, alluvial fans in the wedge-top basin prolongs the river response time to externally forced changes in sediment availability by buffering the hillslope-tributary to trunk river sediment transfer.

These larger landforms buffer at timescales of 10^3-10^6 yr (Fig. 8b; Mather et al., 2017), which overlaps with the timescale of Milankovitch-forced climatic fluctuations.

In comparison, sediment supplied to the river channel is reworked through fluvial processes in narrower valleys. Tributary fans and debris cones, more commonly found such narrow valleys, affect channel conditions over timescales of < 10^4 yr (Fig. 8b; Mather et al., 2017). In the confined 150 – 650 m wide valley of the Bou Tharar reach, terraces preserve only stratified conglomerates characteristic of braided fluvial channel bars and bedforms with a minimum water depth of three meters (Section 4.2; Supporting Information S2). In this case, any input from hillslopes has been reworked by fluvial transport.

These observations demonstrate that lithological and structural controls on valley morphology influence the degree of buffering between hillslope sediment generation and the river channel. As well as the extent to which the river transports and reworks stochastic gravity deposits originating from lateral sources. Consequently, lithological and structural control on both longitudinal and lateral sediment flux into river channels affects the sensitivity of river reaches to external perturbations, such as climate and internal dynamics spurred on by stochastic events. Stochastic sediment supply to river channels can induce local knickpoints and terrace formation, as sediment deposition during a period of bedrock incision can create a local armour layer temporarily pausing further incision (Korup, 2006; Korup et al., 2010; Ouimet et al., 2009; Scherler et al., 2016; Sklar and Dietrich, 2001).

Understanding these concepts is important because constraining spatial and temporal timescales of internal dynamics in sediment supply and transport has been described a high priority aim by Scheingross et al. (2020), with the intent to help signals of internal dynamics to be distinguished from external perturbations. Recognising that the timescales of internal dynamics and sensitivity of river channel sediment supply to external perturbations depend on the underlying conditions of lithology and structure will help guide future research.

5.3 Hard rock gorges isolate river reaches

So far, sediment grain-size, clast lithology and terrace facies have demonstrated that channel sediment content is dependent on local hillslope, tributary and alluvial fan sources (Section 5.1) which have their own connectivity, or response-time to external perturbations, depending on valley width (Section 5.2). Consequently, river incision could occur in any one place along the river at different times. However, to understand how incision starting in one river reach affects the rest of the river, we need to reconstruct the longitudinal profile evolution of the Mgoun River.

The river long profile, strath treads, and terrace abandonment ages (Fig. 5) allow us to identify river profile evolution through knickpoint migration. Numerous field studies have demonstrated terrace formation through progressive knickpoint incision in response to tectonically generated propagating knickpoints (Seidl and Dietrich, 1992; Howard et al., 1994; Zaprowski et al., 2001; Jansen et al., 2011). In these examples, terraces display a diachronous pattern, defined as a pattern of younging upstream. The subsequent conceptual model of knickpoints propagating upstream from downstream perturbations of sea level or tectonic faults to form terrace treads (Finnegan, 2013) has led to further field evidence, dating, and discussion on climatic modulation of tectonically generated knickpoint migration resulting in diachronous terraces (Anthony and Granger, 2007; Baynes et al., 2015; Beckers et al., 2015; Demoulin et al., 2017; DiBiase et al., 2015; Ortega-Becerril et al., 2018; Rixhon et al., 2011). However, the Mgoun River's geomorphic and chronologic evidence challenges this simple model of a base-level generated knickpoint propagation of bedrock incision and terrace abandonment.

Physical experiments by Baynes et al. (2018) have previously shown that rivers can nucleate terrace incision and form local bedrock knickpoints in response to changes in

sediment flux, without dependence on downstream perturbations in base level. This opens up the possibility for incision to start independently at multiple points along the length of a river. This process is more likely when sediment flux histories differ between river reaches, such as along the Mgoun River (see sections 5.1 & 5.2). Knickpoints generated through changes in sediment flux would have a significantly smaller elevation signal than those of tectonically-generated knickpoints. In the Mgoun River, strath formation occurs at ~ 10 – 40 m height on the order of 10^4-10^5 years (Fig. 5), contrasting with the scale of knickpoints created by tectonic perturbations, often exhibiting a few hundred to thousand meters relief depending on the rate of baselevel fall, on the order of 10^6 years (e.g. Boulton et al., 2014) in the High Atlas. We therefore suggest such local knickpoints may be easily overlooked due to their smaller magnitude and will need high resolution DEM data such as the TanDEMx 12 m data used here. In addition, it may be necessary to record both top of terrace surface as well as bedrock strath to construct terrace treads at this scale, with younging of terrace abandonment ages helping to identify the presence of propagating knickpoints (Fig. 5).

Evidence supporting the idea of (1) small magnitude knickpoint propagation and (2) incision starting independently along multiple points along the length of the river can be found in the combination of terrace treads and terrace abandonment ages presented in Figure 5. The younging of abandonment ages upstream and unfinished propagation of terrace abandonment initiated at 105 ka in the thrust front (Fig. 5) demonstrates an erosional disconnect between river reaches in the thrust front and the wedge-top basin since that time. While knickpoint migration from the thrust front is expected to eventually reach the wedge-top basin sometime in the future, the terrace abandonment of the stratigraphic T2 level at 57 ka and T1 after that in the wedge-top basin are likely a product of incision that started independently from the river history downstream in the thrust front.

Whilst the distinct lithological control on sediment flux in each reach between the thrust front and wedge-top basin (see sections 5.1 and 5.2) contribute to the difference in local forcing of incision versus aggradation (Fig. 8), the gorges in hard rock keep the reaches erosionally disconnected (Fig. 5). The locally forced incision could only have been recognised because knickpoint propagation between the thrust front and wedge-top basin was slower than the difference in timing of locally-forced incision ($\Delta t_{knick} > \Delta t_{nucl}$: Fig. 9). Without the hard rock gorges along the course of the Mgoun River, the river profile and terrace abandonment ages would not have expressed the intrinsic dynamics of river incision (Fig. 9).

In the Mgoun River, a wave of incision through knickpoint propagation occurs along a 30 km stretch over a timescale of 10^5 years. Consequently, at timescales of less than 10^5 years, the river was able to respond locally to changes in sediment flux and initiate river incision independently from other sections of the river over a distance of >30 km. Rock erodibility significantly influences the timescales and processes of river long profile evolution, and previously knickpoint celerity has been shown to be affected up to an order of magnitude for a twofold difference in rock strength (Zondervan et al., 2020). Taking into account the substantial difference in rock strength, up to an order of magnitude between the erodible red beds and the resistant limestones along the Mgoun River (Table 1), we anticipate that the gorges of resistant bedrock have been responsible for extending the time needed for knickpoints to propagate (Δt_{knick}) between the Ait Said reach in the thrust front and the wedge-top basin to more than 10^5 yr. While a catchment existing solely of resistant bedrock would also have a slow knickpoint propagation rate (high Δt_{knick}), a preserved terrace record is most likely in weaker lithologies which enable lateral erosion (Montgomery, 2004; Schanz and Montgomery, 2016; Stokes et al., 2017) and consequently also a high speed of knickpoint propagation (low Δt_{knick}). In this context, the most likely landscape to resolve separate nucleations of river incision in the terrace record includes weak bedrock separated by high-strength gorges where $\Delta t_{knick} > \Delta t_{nucl}$.

The discussion so far has demonstrated that bedrock strength of the underlying lithologies and their stratigraphic and structural configuration in a mountain belt affect not only the formation and preservation of strath terrace staircases (e.g. Stokes et al., 2017), but also the timing of terrace formation. The effect of resistant bedrock is not just to slow landscape response in the form of knickpoint propagation (Zondervan et al., 2020), but also to cause low erosional connectivity, fragmenting river reaches that respond to climate in separate ways (Fig. 9). Therefore, especially along long rivers with reaches of resistant bedrock, it is likely that histories of incision and aggradation are asynchronous. Consequently, studies that attempt to constrain river incision by dating terrace staircases in one reach of a river may not accurately represent the river's entire history of incision.

5.4 Where do internal dynamics drive terrace formation?

The impact of lithology and structure is expected to be most pronounced when there are substantial contrasts in bedrock erodibility, which typically occurs during erosion of sedimentary units in thin-skinned tectonic settings often found at the thrust front of a collisional mountain belt (Zondervan et al. 2020a). Additionally, the influence of lateral sediment flux and local valley conditions becomes more crucial when the ratio of longitudinal sediment flux to lateral sediment flux is lowest (Fig. 10). The recycling of conglomerates in thin-skinned thrust front settings (Dingle et al., 2016; Quick et al., 2019), further increases the likelihood of lateral sediment fluxes contributing to asynchronous terrace formation. Thus, along rivers with reaches of resistant bedrock and overall lower rates of rock uplift and incision, asynchronous histories of incision and aggradation are more likely. In contrast to non-glaciated arid to semi-arid settings, mountain belts in temperate settings experiencing ice sheets during glacial periods are more likely to have sediment flux dominated by sourcing from the catchment headwaters and high longitudinal connectivity (Fig. 10). While climatically controlled river terrace staircases are more likely to occur in these glaciated catchments (Bridgland and Westaway, 2008, 2014; Gibbard and Lewin, 2009; Vandenberghe, 1995, 2002, 2003), we recommend caution in extrapolating concepts derived from such examples without due consideration of geomorphic and lithological context.

Finally, the idea that internal dynamics in the wedge-top basin and thrust front can complicate interpretation of climatic and tectonic signals in strath terraces also has implications for depositional settings further downstream. The sediment flux signal exiting the erosional zone of the mountain belt influences the stratigraphy of any subsequent deposition, such as in the foreland basin. Models of alluvial river sediment transfer suggest Milankovitch-scale signals of less than a few hundred thousand years are unlikely to propagate from mountain source areas through alluvial river systems longer than 300 km, due to long intrinsic equilibrium timescales of the sedimentary system (Armitage et al., 2013; Castelltort and Van Den Driessche, 2003; Romans et al., 2016). However, the non-linear and intrinsic dynamics of erosional geomorphic systems on Milankovitch timescales as demonstrated here may lead to fragmented and asynchronous depositional records in more proximal settings like foreland basins (e.g., Foster et al., 2017). The length of a river reach where lithology enhances internal dynamics could affect degree of fragmentation before the signals reaches depositional settings. Investigations aimed at determining the factors influencing internal dynamics in depositional settings would be more effective if paired with an understanding of the extent to which the signals originating from the upstream mountain belt have been fragmented.

Conclusions

Our study of the Mgoun River in Morocco reveals lithology and structure significantly contribute to asynchronous strath terrace formation over 10^4-10^5 year timescales. Recycling of bedrock conglomerates has contributed to a dominance of local hillslope-generated sediment flux. The importance of local hillslope-derived sediment flux in turn

increased the effect of variable valley width set by the stratigraphic and structural configuration of rock strength: valley widths significantly affect sediment connectivity and river-hillslope coupling timescales. The resultant strath terraces formed in reaches of weak bedrock separated by erosion-resistant gorges, resulting in both diachronous and asynchronous patterns of terrace staircase ages. Researchers must carefully evaluate lithological context to discern the relative influences and timescales of internal versus external forcing of terrace formation. Sediment flux and erosional connectivity can significantly vary with lithology and its spatial configuration in the landscape. Accounting for lithology is also key when assessing terrace levels within catchments, as the expectation of constant age versus elevation above the river or smooth younging upstream may not hold where resistant lithologies cause fragmented, asynchronous incision histories between reaches. Similarly, for this reason lithology must factor into dating approaches of terrace staircases and resultant interpretations of river incision rates. These findings reveal lithology modulates internal dynamics, challenging interpretations of strath terrace formation solely linked to climate or tectonic signals, with implications for connected downstream depositional environments.

Supporting Information

Supporting information (pdf)

More detail on river long profile and terrace treads

More detail on terrace sedimentology and interpretation

Tables S1 to S2

Figures S1 to S11

Terrace Field Data - Grain size, Clast Lithological Data & Elevations (Excel file)

DEM Derived Data - River Profile and Terrace Elevations (Excel file)

Schmidt Hammer Rebound Values (Excel file)

References cited

Anthony DM and Granger DE (2007). An empirical stream power formulation for knickpoint retreat in Appalachian Plateau fluviokarst. Journal of Hydrology 343: 117-126. https://doi.org/10.1016/j.jhydrol.2007.06.013

Arboleya ML, Babault J, Owen LA, Teixell A and Finkel RC (2008). Timing and nature of Quaternary fluvial incision in the Ouarzazate foreland basin, Morocco. Journal of the Geological Society 165: 1059-1073. https://doi.org/10.1144/0016-76492007-151

Armitage JJ, Dunkley Jones T, Duller RA, Whittaker AC and Allen PA (2013). Temporal buffering of climate-driven sediment flux cycles by transient catchment response. Earth and Planetary Science Letters 369-370: 200-210. https://doi.org/10.1016/j.epsl.2013.03.020

Attal M and Lavé J (2006). Changes of bedload characteristics along the Marsyandi River (central Nepal): Implications for understanding hillslope sediment supply, sediment load evolution along fluvial networks, and denudation in active orogenic belts. In: Willett SD, Hovius N, Brandon MT, Fisher DM, (Eds.), Tectonics, Climate, and Landscape Evolution. Geological Society of America. https://doi.org/10.1130/2006.2398(09)

Babault J, Teixell A, Arboleya ML and Charroud M (2008). A Late Cenozoic age for long-wavelength surface uplift of the Atlas Mountains of Morocco. Terra Nova 20: 102-107. https://doi.org/10.1111/j.1365-3121.2008.00794.x

Baynes ERC, Attal M, Niedermann S, Kirstein LA, Dugmore AJ and Naylor M (2015). Erosion during extreme flood events dominates Holocene canyon evolution in northeast Iceland. Proceedings of the National Academy of Sciences 112: 2355-2360. https://doi.org/10.1073/pnas.1415443112

Baynes ERC, Lague D and Kermarrec J-J (2018). Supercritical river terraces generated by hydraulic and geomorphic interactions. Geology 46: 499-502. https://doi.org/10.1130/G40071.1

Beckers A, Bovy B, Hallot E and Demoulin A (2015). Controls on knickpoint migration in a drainage network of the moderately uplifted Ardennes Plateau, Western Europe. Earth Surface Processes and Landforms 40: 357-374. https://doi.org/10.1002/esp.3638

Boulton SJ, Stokes M (2018). Which DEM is best for analyzing fluvial landscape development in mountainous terrains? Geomorphology 310: 168-187. https://doi.org/10.1016/j.geomorph.2018.03.002

Boulton SJ, Stokes M and Mather AE (2014). Transient fluvial incision as an indicator of active faulting and Plio-Quaternary uplift of the Moroccan High Atlas. Tectonophysics 633: 16-33. https://doi.org/10.1016/j.tecto.2014.06.032

Boulton SJ, VanDeVelde JH and Grimes ST (2019). Palaeoenvironmental and tectonic significance of Miocene lacustrine and palustrine carbonates (Ait Kandoula Formation) in the Ouarzazate Foreland Basin, Morocco. Sedimentary Geology 383: 195-215. https://doi.org/10.1016/j.sedgeo.2019.01.009

Bridgland DR and Westaway R (2008). Climatically controlled river terrace staircases: A worldwide Quaternary phenomenon. Geomorphology 98: 285-315. https://doi.org/10.1016/j.geomorph.2006.12.032

Bridgland DR and Westaway R (2014). Quaternary fluvial archives and landscape evolution: a global synthesis. Proceedings of the Geologists' Association 125: 600-629. https://doi.org/10.1016/j.pgeola.2014.10.009

Brozovic N and Burbank DW (2000). Dynamic fluvial systems and gravel progradation in the Himalayan foreland. GSA Bulletin 112: 394-412. https://doi.org/10.1130/0016-7606(2000)112%3C394:DFSAGP%3E2.0.CO;2

Burbank DW and Anderson RS (2011). Tectonic geomorphology. John Wiley & Sons. https://doi.org/10.1002/9781444345063

Cappy S (2006). Hydrogeological characterization of the Upper Draa catchment: Morocco. Unpublished PhD thesis, Geological Institute, Faculty of Mathematics and Natural Sciences, University of Bonn.

Carte Géologique du Maroc, (1975). Jbel Saghro-Dadès.

Castelltort S and Van Den Driessche J (2003). How plausible are high-frequency sediment supply-driven cycles in the stratigraphic record? Sedimentary Geology 157: 3-13. https://doi.org/10.1016/S0037-0738(03)00066-6

Chellai EH and Perriaux J (1996). Evolution geodynamique d'un bassin d'avant-pays du domaine atlasique (Maroc): exemple des depots neogenes et quaternaires du versant septentrional de l'Atlas de Marrakech. Comptes rendus de l'Académie des sciences. Série 2. Sciences de la terre et des planètes 322(9): 727-734.

Cordier S, Briant B, Bridgland D, Herget J, Maddy D, Mather A and Vandenberghe J (2017). The Fluvial Archives Group: 20 years of research connecting fluvial

geomorphology and palaeoenvironments. Quaternary Science Reviews 166: 1-9. https://doi.org/10.1016/j.quascirev.2017.03.001

DiBiase RA, Whipple KX, Lamb MP and Heimsath AM (2015). The role of waterfalls and knickzones in controlling the style and pace of landscape adjustment in the western San Gabriel Mountains, California. GSA Bulletin 127: 539-559. https://doi.org/10.1130/b31113.1

de Jong C, Cappy S, Finckh M and Funk D (2008). A transdisciplinary analysis of water problems in the mountainous karst areas of Morocco. Engineering Geology 99: 228-238.

Demoulin A, Mather A and Whittaker A (2017). Fluvial archives, a valuable record of vertical crustal deformation. Quaternary Science Reviews 166: 10-37. https://doi.org/10.1016/j.quascirev.2016.11.011

Dingle EH, Sinclair HD, Attal M, Milodowski DT and Singh V (2016). Subsidence control on river morphology and grain size in the Ganga Plain. American Journal of Science 316: 778-812. https://doi.org/10.2475/08.2016.03

Dixit Y, Toucanne S, Fontanier C, Pasquier V, Lora JM, Jouet G and Tripati A (2020). Enhanced western Mediterranean rainfall during past interglacials driven by North Atlantic pressure changes. Quaternary International 553: 1-13. https://doi.org/10.1016/j.quaint.2020.08.017

Dłużewski M, Krzemień K, Rojan E and Biejat K (2013). Stream channel development in the southern parts of the High Atlas Mountains, Morocco. Geografija 49.

Dubille M and Lavé J (2015). Rapid grain size coarsening at sandstone/conglomerate transition: similar expression in Himalayan modern rivers and Pliocene molasse deposits. Basin Research 27: 26-42. https://doi.org/10.1111/bre.12071

Duller RA, Whittaker AC, Fedele JJ, Whitchurch AL, Springett J, Smithells R, Fordyce S and Allen PA (2010). From grain size to tectonics. Journal of Geophysical Research 115. https://doi.org/10.1029/2009JF001495

El Harfi A, Lang J, Salomon J and Chellai E (2001). Cenozoic sedimentary dynamics of the Ouarzazate foreland basin (central High Atlas Mountains, Morocco). International Journal of Earth Sciences 90: 393-411. https://doi.org/10.1007/s005310000115

Fedele JJ and Paola C (2007). Similarity solutions for fluvial sediment fining by selective deposition. Journal of Geophysical Research: Earth Surface 112. https://doi.org/10.1029/2005JF000409

Ferguson R, Hoey T, Wathen S and Werritty A (1996). Field evidence for rapid downstream fining of river gravels through selective transport. Geology 24: 179-182. https://doi.org/10.1130/0091-7613(1996)024%3C0179:FEFRDF%3E2.3.CO;2

Fink AH and Knippertz P (2003). An extreme precipitation event in southern Morocco in spring 2002 and some hydrological implications. Weather 58: 377-387.

Finnegan NJ (2013). Interpretation and downstream correlation of bedrock river terrace treads created from propagating knickpoints. Journal of Geophysical Research: Earth Surface 118: 54-64. https://doi.org/10.1029/2012JF002534

Finnegan NJ and Balco G (2013). Sediment supply, base level, braiding, and bedrock river terrace formation: Arroyo Seco, California, USA. Geological Society of America Bulletin 125(7-8): 1114-1124. https://doi.org/10.1130/B30727.1

Finnegan NJ and Dietrich WE (2011). Episodic bedrock strath terrace formation due to meander migration and cutoff. Geology 39(2): 143-146. https://doi.org/10.1130/G31716.1

Finnegan NJ, Schumer R and Finnegan S (2014). A signature of transience in bedrock river incision rates over timescales of 10^4–10^7 years. Nature 505: 391-394. https://doi.org/10.1038/nature12913

Foster MA, Anderson RS, Gray HJ and Mahan SA (2017). Dating of river terraces along Lefthand Creek, western High Plains, Colorado, reveals punctuated incision. Geomorphology 295: 176-190. https://doi.org/10.1016/j.geomorph.2017.04.044

Fryirs K (2013). (Dis)Connectivity in catchment sediment cascades: A fresh look at the sediment delivery problem. Earth Surface Processes and Landforms 38: 30-46. https://doi.org/10.1002/esp.3242

Fryirs KA, Brierley GJ, Preston NJ and Kasai M (2007). Buffers, barriers and blankets: The (dis)connectivity of catchment-scale sediment cascades. CATENA 70: 49-67. https://doi.org/10.1016/j.catena.2006.07.007

Fuller TK, Perg LA, Willenbring JK and Lepper K (2009). Field evidence for climate-driven changes in sediment supply leading to strath terrace formation. Geology 37(5): 467-470. https://doi.org/10.1130/G25487A.1

Gibbard PL and Lewin J (2009). River incision and terrace formation in the Late Cenozoic of Europe. Tectonophysics 474: 41-55. https://doi.org/10.1016/j.tecto.2008.11.017

Gomez F, Beauchamp W and Barazangi M (2000). Role of the Atlas Mountains (northwest Africa) within the African-Eurasian plate-boundary zone. Geology 28(9): 775-778. https://doi.org/10.1130/0091-7613(2000)28%3C775:ROTAMN%3E2.0.CO;2

Goudie AS (2006). The Schmidt Hammer in geomorphological research. Progress in Physical Geography: Earth and Environment 30: 703-718. https://doi.org/10.1177/0309133306071954

Grimaud J-L, Paola C and Voller V (2016). Experimental migration of knickpoints: influence of style of base-level fall and bed lithology. Earth Surface Dynamics 4(1): 11-23. https://doi.org/10.5194/esurf-4-11-2016

Hancock GS and Anderson RS (2002). Numerical modeling of fluvial strath-terrace formation in response to oscillating climate. GSA Bulletin 114: 1131-1142. https://doi.org/10.1130/0016-7606(2002)114<1131:NMOFST>2.0.CO;2

Howard AD, Dietrich WE and Seidl MA (1994). Modeling fluvial erosion on regional to continental scales. Journal of Geophysical Research: Solid Earth 99: 13971-13986. https://doi.org/10.1029/94JB00744

Jansen JD, Fabel D, Bishop P, Xu S, Schnabel C and Codilean AT (2011). Does decreasing paraglacial sediment supply slow knickpoint retreat? Geology 39: 543-546. https://doi.org/10.1130/G32018.1

Knippertz P (2003). Tropical–Extratropical Interactions Causing Precipitation in Northwest Africa: Statistical Analysis and Seasonal Variations. Monthly Weather Review 131: 3069-3076. https://doi.org/10.1175/1520-0493(2003)131%3C3069:TICPIN%3E2.0.CO;2

Knippertz P, Fink AH, Reiner A and Speth P (2003). Three Late Summer/Early Autumn Cases of Tropical–Extratropical Interactions Causing Precipitation in Northwest Africa. Monthly Weather Review 131: 116-135. https://doi.org/10.1175/1520-0493(2003)131%3C0116:TLSEAC%3E2.0.CO;2

Komar PD and Li Z (1986). Pivoting analyses of the selective entrainment of sediments by shape and size with application to gravel threshold. Sedimentology 33: 425-436. https://doi.org/10.1111/j.1365-3091.1986.tb00546.x

Korup O (2006). Rock-slope failure and the river long profile. Geology 34: 45-48. https://doi.org/10.1130/G21959.1

Korup O, Densmore AL and Schlunegger F (2010). The role of landslides in mountain range evolution. Geomorphology 120: 77-90. https://doi.org/10.1016/j.geomorph.2009.09.017

Larrasoaña JC, Roberts AP and Rohling EJ (2013). Dynamics of Green Sahara Periods and Their Role in Hominin Evolution. PLOS ONE 8, e76514. https://doi.org/10.1371/journal.pone.0076514

Lavé J and Avouac JP (2000). Active folding of fluvial terraces across the Siwaliks Hills, Himalayas of central Nepal. Journal of Geophysical Research: Solid Earth 105(B3): 5735-5770. https://doi.org/10.1029/1999JB900292

Leopold LB, Wolman MG and Miller JP (1964). Fluvial Processes in Geomorphology. Freeman, San Francisco, 522 p.

Limaye AB and Lamb MP (2016). Numerical model predictions of autogenic fluvial terraces and comparison to climate change expectations. Journal of Geophysical Research: Earth Surface 121(3): 512-544. https://doi.org/10.1002/2014JF003392

Mather AE, Stokes M and Whitfield E (2017). River terraces and alluvial fans: The case for an integrated Quaternary fluvial archive. Quaternary Science Reviews 166: 74-90. https://doi.org/10.1016/j.quascirev.2016.09.022

Mather AE and Stokes M (2018). Bedrock structural control on catchment-scale connectivity and alluvial fan processes, High Atlas Mountains, Morocco. Geological Society, London, Special Publications 440: 103-128. https://doi.org/10.1144/SP440.15

Miall AD (1978). Lithofacies types and vertical profile models in braided river deposits: A summary. In: Miall AD, (Ed.), Fluvial Sedimentology. Canadian Society of Petroleum Geologists.

Montgomery DR (2004). Observations on the role of lithology in strath terrace formation and bedrock channel width. American Journal of Science 304: 454-476.

Ortega-Becerril JA, Garzón G, Tejero R, Meriaux A-S, Delunel R, Merchel S and Rugel G (2018). Controls on strath terrace formation and evolution: The lower Guadiana River, Pulo do Lobo, Portugal. Geomorphology 319: 62-77. https://doi.org/10.1016/j.geomorph.2018.07.015

Ouimet WB, Whipple KX and Granger DE (2009). Beyond threshold hillslopes: Channel adjustment to base-level fall in tectonically active mountain ranges. Geology 37: 579-582. https://doi.org/10.1130/G30013A.1

Paola C, Parker G, Seal R, Sinha SK, Southard JB and Wilcock PR (1992). Downstream Fining by Selective Deposition in a Laboratory Flume. Science 258: 1757-1760. https://doi.org/10.1126/science.258.5089.1757

Pastor A, Babault J, Teixell A and Arboleya ML (2012). Intrinsic stream-capture control of stepped fan pediments in the High Atlas piedmont of Ouarzazate (Morocco). Geomorphology 173-174: 88-103. https://doi.org/10.1016/j.geomorph.2012.05.032

Pazzaglia FJ (2013). Fluvial terraces. In: Shroder JF, ed. Treatise on Geomorphology. Academic Press, pp.379-412.

Quick L, Sinclair HD, Attal M and Singh V (2019). Conglomerate recycling in the Himalayan foreland basin: Implications for grain size and provenance. GSA Bulletin 132: 1639-1656. https://doi.org/10.1130/B35334.1

Rice SP and Church M (2001). Longitudinal profiles in simple alluvial systems. Water Resources Research 37: 417-426. https://doi.org/10.1029/2000WR900266

Rixhon G, Braucher R, Bourlès D, Siame L, Bovy B and Demoulin A (2011). Quaternary river incision in NE Ardennes (Belgium)–Insights from 10Be/26Al dating

of river terraces. Quaternary Geochronology 6: 273-284. https://doi.org/10.1016/j.quageo.2010.11.001

Romans BW, Castelltort S, Covault JA, Fildani A and Walsh JP (2016). Environmental signal propagation in sedimentary systems across timescales. Earth-Science Reviews 153: 7-29. https://doi.org/10.1016/j.earscirev.2015.07.012

Schanz SA and Montgomery DR (2016). Lithologic controls on valley width and strath terrace formation. Geomorphology 258: 58-68. https://doi.org/10.1016/j.geomorph.2016.01.015

Schanz SA, Montgomery DR, Collins BD and Duvall AR (2018). Multiple paths to straths: A review and reassessment of terrace genesis. Geomorphology 312: 12-23. https://doi.org/10.1016/j.geomorph.2018.03.028

Scheingross JS, Limaye AB, McCoy SW and Whittaker AC (2020). The shaping of erosional landscapes by internal dynamics. Nature Reviews Earth & Environment. https://doi.org/10.1038/s43017-020-0096-0

Scherler D, Lamb MP, Rhodes EJ and Avouac J-P (2016). Climate-change versus landslide origin of fill terraces in a rapidly eroding bedrock landscape: San Gabriel River, California. GSA Bulletin 128: 1228-1248. https://doi.org/10.1130/B31356.1

Schulz O, Busche H and Benbouziane A (2008). Decadal Precipitation Variances and Reservoir Inflow in the Semi-Arid Upper Drâa Basin (South-Eastern Morocco), in Zereini F, Hötzl H, eds. Climatic Changes and Water Resources in the Middle East and North Africa. Springer Berlin Heidelberg, Berlin, Heidelberg, pp. 165-178.

Seidl MA, Dietrich WE, Schmidt KH and De Ploey J (1992). The problem of channel erosion into bedrock. Functional geomorphology 23: 101-124.

Simpson G and Castelltort S (2012). Model shows that rivers transmit high-frequency climate cycles to the sedimentary record. Geology 40: 1131-1134. https://doi.org/10.1130/G33451.1

Sklar LS and Dietrich WE (2001). Sediment and rock strength controls on river incision into bedrock. Geology 29: 1087-1090. https://doi.org/10.1130/0091-7613(2001)029%3C1087:SARSCO%3E2.0.CO;2

Spotila JA and Prince PS (2022). Geomorphic complexity and the case for topographic rejuvenation of the Appalachian Mountains. Geomorphology. https://doi.org/10.1016/j.geomorph.2022.108449

Starkel L (2003). Climatically controlled terraces in uplifting mountain areas. Quaternary Science Reviews 22(20): 2189-2198. https://doi.org/10.1016/S0277-3791(03)00148-3

Sternberg H (1875). Untersuchungen über längen-und querprofil geschiebeführender flüsse. Zeitshrift für Bauwesen 25: 483-506.

Stokes M, Cunha PP and Martins AA (2012). Techniques for analysing Late Cenozoic river terrace sequences. Geomorphology 165–166: 1-6. http://dx.doi.org/10.1016/j.geomorph.2012.03.022

Stokes M and Mather AE (2015). Controls on modern tributary-junction alluvial fan occurrence and morphology: High Atlas Mountains, Morocco. Geomorphology 248: 344-362. https://doi.org/10.1016/j.geomorph.2015.08.003

Stokes M, Mather AE, Belfoul M, Faik F, Bouzid S, Geach MR, Cunha PP, Boulton SJ and Thiel C (2017). Controls on dryland mountain landscape development along the NW Saharan desert margin: Insights from Quaternary river terrace sequences (Dadès River, south-central High Atlas, Morocco). Quaternary Science Reviews 166: 363-379. https://doi.org/10.1016/j.quascirev.2017.04.017

Tadono T, Ishida H, Oda F, Naito S, Minakawa K and Iwamoto H (2014). Precise global DEM generation by ALOS PRISM. ISPRS Annals of the Photogrammetry, Remote Sensing and Spatial Information Sciences 2: 71. https://doi.org/10.5194/isprsannals-II-4-71-2014

Tesón E, Pueyo EL, Teixell A, Barnolas A, Agustí J and Furió M (2010). Magnetostratigraphy of the Ouarzazate Basin: Implications for the timing of deformation and mountain building in the High Atlas Mountains of Morocco. Geodinamica Acta 23: 151-165. https://doi.org/10.3166/ga.23.151-165

Tesón E and Teixell A (2008). Sequence of thrusting and syntectonic sedimentation in the eastern Sub-Atlas thrust belt (Dadès and Mgoun valleys, Morocco). International Journal of Earth Sciences 97: 103-113. https://doi.org/10.1007/s00531-006-0151-1

Tjallingii R, Claussen M, Stuut J-BW, Fohlmeister J, Jahn A, Bickert T, Lamy F and Röhl U (2008). Coherent high- and low-latitude control of the northwest African hydrological balance. Nature Geoscience 1: 670. https://doi.org/10.1038/ngeo289

Vandenberghe J (1995). Timescales, climate and river development. Quaternary Science Reviews 14: 631-638. https://doi.org/10.1016/0277-3791(95)00043-O

Vandenberghe J (2002). The relation between climate and river processes, landforms and deposits during the Quaternary. Quaternary International 91: 17-23. https://doi.org/10.1016/S1040-6182(01)00098-2

Vandenberghe J (2003). Climate forcing of fluvial system development: an evolution of ideas. Quaternary Science Reviews 22: 2053-2060. https://doi.org/10.1016/S0277-3791(03)00213-0

Watkins SE, Whittaker AC, Bell RE, Brooke SA, Ganti V, Gawthorpe RL, McNeill LC and Nixon CW (2020). Straight from the source's mouth: Controls on field-constrained sediment export across the entire active Corinth Rift, central Greece. Basin Research 32: 1600-1625. https://doi.org/10.1111/bre.12444

Whipple KX, DiBiase RA and Crosby BT (2013). Bedrock rivers. In: Fluvial geomorphology. Elsevier Inc., pp. 550-573. http://dx.doi.org/10.1016/B978-0-12-374739-6.00254-2

Whittaker AC, Attal M and Allen PA (2010). Characterising the origin, nature and fate of sediment exported from catchments perturbed by active tectonics. Basin Research 22: 809-828. https://doi.org/10.1111/j.1365-2117.2009.00447.x

Whittaker AC and Boulton SJ (2012). Tectonic and climatic controls on knickpoint retreat rates and landscape response times. Journal of Geophysical Research: Earth Surface 117. https://doi.org/10.1029/2011JF002157

Whittaker AC, Cowie PA, Attal M, Tucker GE and Roberts GP (2007a). Bedrock channel adjustment to tectonic forcing: Implications for predicting river incision rates. Geology 35: 103-106. https://doi.org/10.1130/G23106A.1

Whittaker AC, Duller RA, Springett J, Smithells RA, Whitchurch AL and Allen PA (2011). Decoding downstream trends in stratigraphic grain size as a function of tectonic subsidence and sediment supply. GSA Bulletin 123: 1363-1382. https://doi.org/10.1130/B30351.1

Wolman MG (1954). A method of sampling coarse river-bed material. Eos, Transactions American Geophysical Union 35: 951-956. https://doi.org/10.1029/TR035i006p00951

Wolpert JA and Forte AM (2021). Response of transient rock uplift and base level knickpoints to erosional efficiency contrasts in bedrock streams. Earth Surface Processes and Landforms 46(10): 2092-2109. https://doi.org/10.1002/esp.5146

Zaprowski BJ, Evenson EB, Pazzaglia FJ and Epstein JB (2001). Knickzone propagation in the Black Hills and northern High Plains: A different perspective on the late Cenozoic exhumation of the Laramide Rocky Mountains. Geology 29: 547-550. https://doi.org/10.1130/0091-7613(2001)029<0547:Kpitbh>2.0.Co;2

Zondervan JR (2021). Lithological and climatic controls on fluvial landscape evolution of a post-orogenic dryland mountain belt [PhD Thesis]. University of Plymouth, 248 p. https://dx.doi.org/10.24382/1027

Zondervan JR, Stokes M, Boulton SJ, Telfer MW and Mather AE (2020a). Rock strength and structural controls on fluvial erodibility: Implications for drainage divide mobility in a collisional mountain belt: Earth and Planetary Science Letters 538: 116221. https://doi.org/10.1016/j.epsl.2020.116221

Zondervan JR, Stokes M, Boulton SJ, Telfer MW, Mather AE, Buylaert JP, Jain M, Murray AS and Belfoul MA (2022). Constraining a model of punctuated river incision for Quaternary strath terrace formation. Geomorphology 414: 108396. https://doi.org/10.1016/j.geomorph.2022.108396

Zondervan JR, Whittaker AC, Bell RE, Watkins SE, Brooke SA and Hann MG (2020b). New constraints on bedrock erodibility and landscape response times upstream of an active fault. Geomorphology 351: 106937. https://doi.org/10.1016/j.geomorph.2019.106937

Figure Captions

Figure 1. High Atlas and the Mgoun River catchment, where the river crosses several orogenic structures within the sedimentary cover of the mountain belt (c.f. Stokes et al. 2017) before entering the Ouarzazate foreland basin. We examine the strath terrace formation in the study area shown by the inset for Fig. 2, where lithology has a strong control of valley morphology, sediment supply and river erosion. See a comparison with Zondervan et al. (2020a) for the lithological context for the full High Atlas Mountains. Rif = The Rif Mountains.

Figure 2. Geology of the Mgoun River study area from the town of Aifar in the thrust front to Aït Toumert in the wedge-top basin. Ephemeral tributaries are marked in white and the perennial trunk streams in blue. Terraces are marked in black. Map and cross section modified from Carte Géologique du Maroc (1975); Tesón et al. (2010); Tesón and Teixell (2008). See Table 1 for details of lithologies and their rock strength. Geographic coordinates can be found from Fig. 1.

Figure 3. Bedrock geology and geomorphology of the study area, with photos ordered from the uppermost gorge near Aït Toumert in the wedge-top basin, to the most downstream reach in the thrust front up until Aifar. Town names refer to those in Fig. 2. The perennial river trunk flows through at least four valleys formed in weak red beds, separated by gorges made from limestone bedrock. (a) Gorge in strong Jurassic Limestone. (b) Open valley form of the wedge-top basin in the weak Cretaceous red beds bounded on either side by Jurassic strong limestone and mixed-strong limestones and marls. The wide valley accommodates the gradual surfaces of alluvial fans. (c) Gorge in strong Jurassic limestone. (d) Confined valley in weak Eocene red beds bounded by strong Mio-Pliocene conglomerates and Eocene Limestones. (e,f) Gorge in strong Eocene limestones opening up into a confined valley in weak Eocene red beds. (g) Confined valley formed in weak Eocene red beds and bounded by strong Eocene limestones interbedded with weak Cretaceous red beds. (h) River flowing from a confined valley in Eocene red beds into a gorge in strong Eocene limestones. (j) Confined to open valley in weak Eocene red beds bounded by strong Mio-Pliocene conglomerates, weak Mio-Pliocene red beds, and strong Eocene limestones. See Table 1 for details of lithologies and rock strength.

Figure 4. Valley cross-sections of the three river reaches with strath terraces. Sections facing downstream direction. Cross-section lines are displayed in Fig. 2. Oldest and youngest OSL date for fluvial bedload gravels on terraces from Zondervan et al. (2022). (a) Staircase of strath terraces > 1 km wide in the wedge-top basin, overlying weak Cretaceous marls dipping in the direction of the modern river. T2 on the other bank is perched on locally mixed-strong bedrock. (b) Bou Tharar reach in the high relief thrust front with unpaired strath terraces on weak Eocene red beds, with valley walls consisting of strong Eocene limestones. The highest documented terrace is isolated from the rest of the valley by gullies and the modern river channel. (c) Valley of the Ait Saïd reach in the downstream extent of the thrust front with two strath levels, including a wide strath terrace T2 in weak Eocene red beds bordered by Pliocene conglomerates. Slope material from the Pliocene conglomerates lap onto the fluvial gravels of T2.

Figure 5. Terrace treads between gorge-bound reaches. (a) abandonment ages and river profile evolution. Modern river long profile of the Mgoun River with terrace treads and OSL dates of terrace abandonment. More detailed data and sections of this river profile can be found in Supplementary Information Fig. S2. (b) simplified conceptual 3D diagram of the profiles shown in (a). Three reaches with variable number of strath levels. Levels in the most upstream reach are labelled T' to distinguish them as independent from the levels further downstream. Figure S4 in the supporting information is a 3D render of the TanDEMx hillshade which shows the distribution of terraces as shown in this figure.

Figure 6. Overview of terrace sedimentology of the three reaches. (a) In the upstream wedge-top basin: an example of a T2 created by a tributary channel cut-off. The photo shows the section at where the perennial channel floodplain has cut into the terrace. Clast imbrication is towards and along the axial perennial river channel direction. The inversely graded conglomerate (Gci) records sediment gravity flows from the ephemeral tributary into the axial river floodplain. A T2 in a lobe-shaped alluvial fan deposit next to a wide floodplain is characterised by massive clast to matrix supported conglomerate (Gcm) interbedded with tan-coloured sand and mud (Fl). **(b)** Section through terrace T2 in the midstream Bou Tharar reach showing a 10 m thick deposit of bedform conglomerates (Gh) interbedded with trough- stratified minor channel conglomerates (Gt) and planar stratified transverse gravel bar conglomerates (Gp). **(c)** T2 in the downstream Ait Said reach with ten meters of two sequences of graded conglomerate (Gcg) to sand-mud sheets (Fl) and capped with massive angular conglomerates (Gcm). Further details can be found in the Supplementary Information.

Figure 7. Grain size and lithology data along the Mgoun River. (a) Bar plots of the lithological contribution to river terrace gravels and modern river bars (locations with an 'a'). **(b)** Wolman point count results for each terrace and modern-river location, along the length of the surveyed trunk stream. The fining exponents from exponential fits (Eq. 1) are given together with the r-squared values. River channel confluences are marked as open triangles and ephemeral tributaries are marked as black triangles.

Figure 8. Valley width controlled by lithological and passive tectonic structural controls and its effect on sediment flux. (a) Passive structural geology and lithology influence terrace formation in three ways: 1) The presence of structurally exposed conglomerates in certain valleys allows for recycling of clasts into Quaternary valley fill sediments. This effect can influence grain size, as well as the lithological signature and abundance of available sediments within valleys; 2) Spacing of thrusted low erodibility lithologies determines the width of valleys. Wider valleys can accommodate alluvial fans and extensive tributaries. Lateral sediment features buffer the coupling between hillslopes and the river channel in wide valleys, whilst in narrow valleys this coupling is more direct. Furthermore, extensive lateral input means bedload is supplied with coarse-grained sediment, preventing downstream fining. Wider valleys can accommodate the preservation of more terrace levels than narrower valleys. 3) The bedrock erodibility of lithologies along the length of the river influences knickpoint migration speeds. Low

erodibility gorges can act as significant blocks against the propagation and connectivity of terrace treads, keeping terrace formation processes local. **(b)** The typical spatial and temporal scales of distributive fluvial features coupling hillslope sediment generation with river channel transport (from Mather et al. 2017). As valley width increases, features buffering between hillslopes and river channels increase in spatial and temporal scales. At the timescale of terrace formation in the High Atlas, the presence of alluvial fans is expected to make a significant impact on timing of formation.**Figure 9. Conceptual model demonstrating how younging of terrace abandonment ages upstream can be interpreted as either propagation of incision that started downstream versus as incision in river reaches starting at different times independently. (a)** Snapshot of longitudinal profile evolution of a river eroding through erodible bedrock separated by gorges in resistant bedrock at t1. Following 'nucleation' of incision (e.g. Baynes et al., 2018) at a point downstream at t0 (in Reach 1 (R1)), a knickpoint has propagated through one gorge and into the next reach upstream (R2). River incision leading to terrace abandonment has started independently in both the second (R2) and fourth reach (R4) at t1. **(b)** At t2, terrace treads with terrace abandonment ages record the timing of incision along the river. In the second reach (R2), the independent start of incision at t1 cannot be distinguished from the incision which started at t0 downstream, since the knickpoint has propagated through R2. The resultant younging upstream of terrace abandonment ages from R1 to R2 can be interpreted as one initiation of incision propagated by a knickpoint. However, since the knickpoint has not yet reached the fourth reach, one can resolve the initiation of incision at t1 in R4 as independent from the incision downstream. Only if knickpoint propagation is slower than the difference in timing of locally-forced incision ($\Delta t_{knick} > \Delta t_{nucl}$) can locally forced incision be recognised.

Figure 10. Conceptual model of sediment flux from source to sink, in a non-glaciated and glaciated mountain belt. (a) in the non-glaciated model, a trunk river traversing the centre of the mountain belt (including the fold-thrust belt) to its peripheral edges (including wedge-top basins and the thrust front) increases its sediment flux, but lateral input is still relatively large enough to make an impact on local trunk river sediment flux. Once the ratio of lateral sediment fluxes to the trunk sediment flux decreases, the system can be treated as a point-source system. **(b)** in a glaciated environment, glacial activity over glacial-interglacial timescales dominates the sediment flux from a much more central position, and the peripheral mountain regions and foreland basin can be treated as being controlled by a point source. This study is situated in the peripheral mountain region in a non-glaciated setting, where lateral sediment fluxes are important, and where erodibility contrasts elicit dynamics described in sections above.

Tables

Table 1 | Lithostratigraphic packages labelled in Figures 2 and 3, with details of lithologies and rock strength

Formation	Lithologies	N	Schmidt hammer value (mean, stdev)	UCS in MPa (mean, stdev)	Strength[†]
Pliocene conglomerates (P-c)	Continental fluvial conglomerates	50	33, 9	22, 6	Erodible
Mio-Pliocene red beds (MP-r)	Continental fluvial sandstone and siltstone	10	27, 7	14, 4	Very erodible
Mio-Pliocene conglomerate (MP-c)	Continental fluvial and fan conglomerate	-	-	-	Erodible[‡]
Eocene red beds (E-r)	Continental and marine marl	47	22, 15	10, 7	Very erodible
Eocene limestone (E-L)	Marine limestone	64	41, 12	39, 11	Moderately resistant
Cretaceous red marls (C-r)	Continental red sandstone, shale, and gypsum	70	26, 13	14, 7	Very erodible
Jurassic limestones and marls (J-r/L)	Continental and marginal marine silts, marls, sandstone, and limestone	60	43, 16	45, 17	Moderately resistant
Jurassic Limestones (J-L)	Massive marine platform limestone	90	53, 11	90, 18	Resistant

[†]as defined by classifications in Goudie (2006) & Zondervan et al. (2020); [‡]no direct Schmidt readings but similar lithology to P-c

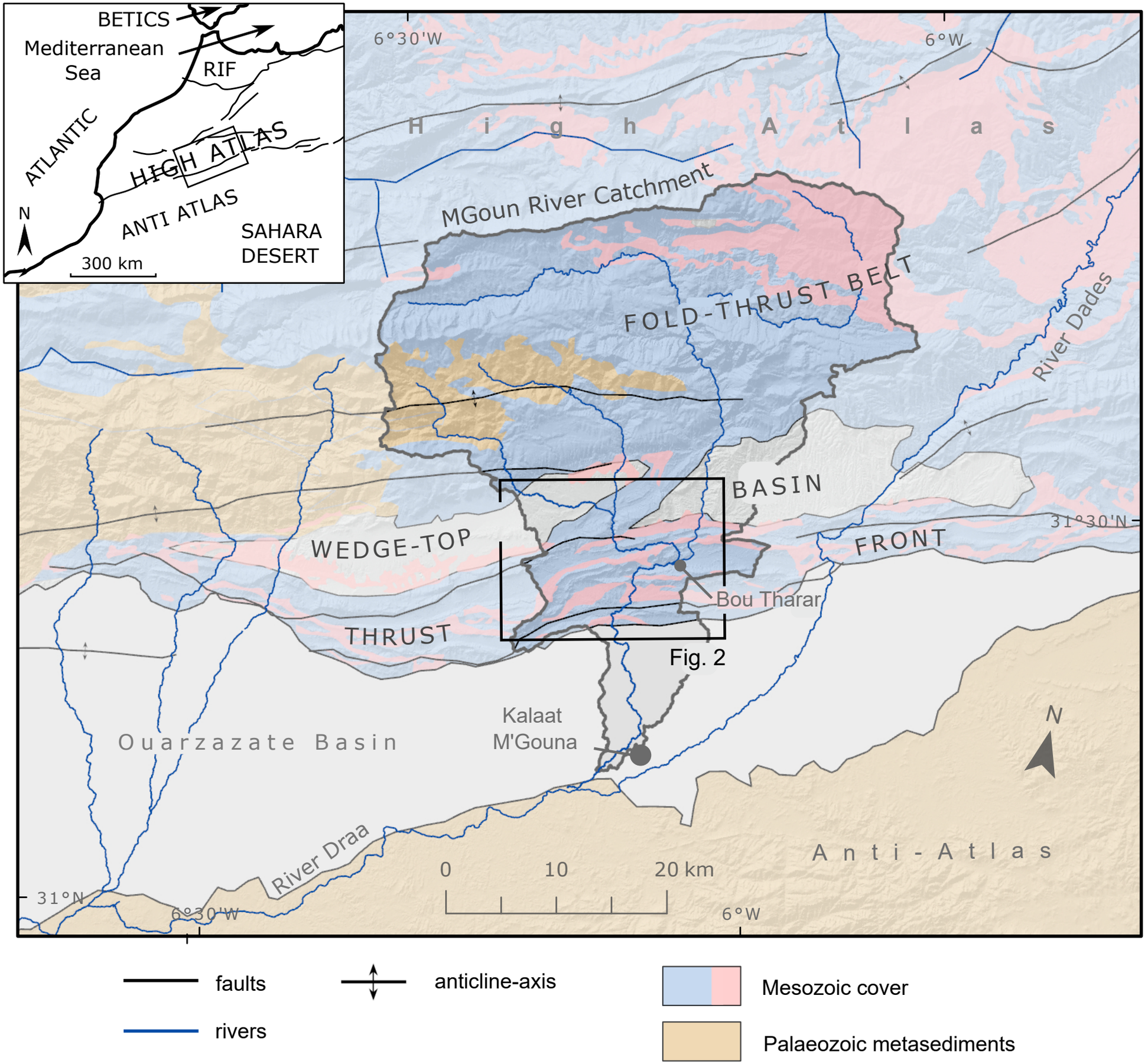
BETICS
Mediterranean Sea
RIF
ATLANTIC
HIGH ATLAS
ANTI ATLAS
SAHARA DESERT
N
300 km
6°30'W
6°W
High Atlas
MGoun River Catchment
FOLD-THRUST BELT
River Dades
BASIN
WEDGE-TOP
FRONT
31°30'N
Bou Tharar
THRUST
Fig. 2
Kalaat M'Gouna
Ouarzazate Basin
N
River Draa
Anti-Atlas
0
10
20 km
31°N
6°30'W
6°W
faults
anticline-axis
Mesozoic cover
rivers
Palaeozoic metasediments

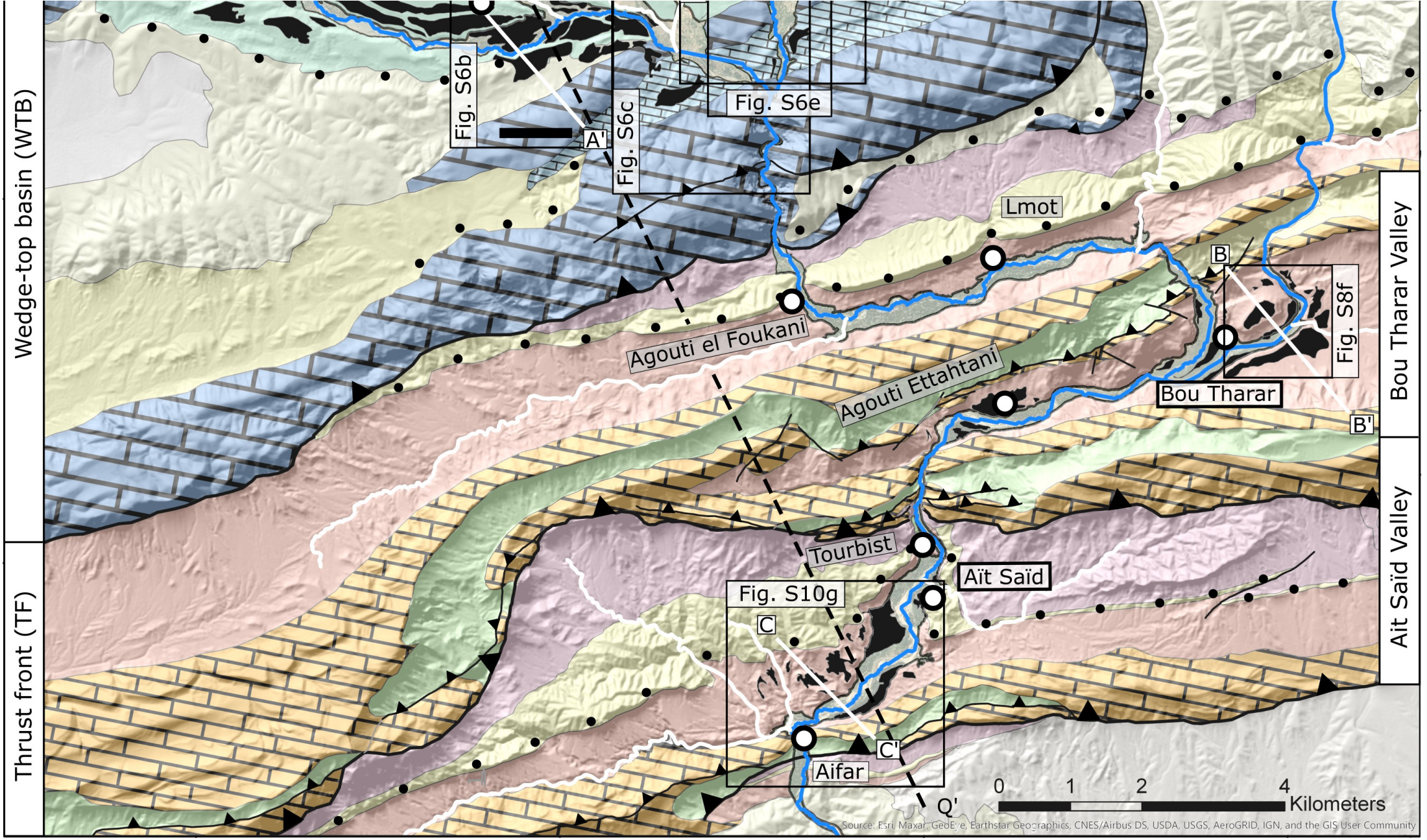
Wedge-top basin (WTB)
Thrust front (TF)
Bou Tharar Valley
Ait Saïd Valley
Fig. S6b
Fig. S6c
Fig. S6e
A'
Lmot
B
Fig. S8f
B'
Agouti el Foukani
Agouti Ettahtani
Bou Tharar
Tourbist
Aït Saïd
Fig. S10g
C
C'
Aifar
Q'
0 1 2 4
Kilometers
Source: Esri, Maxar, GeoEye, Earthstar Geographics, CNES/Airbus DS, USDA, USGS, AeroGRID, IGN, and the GIS User Community

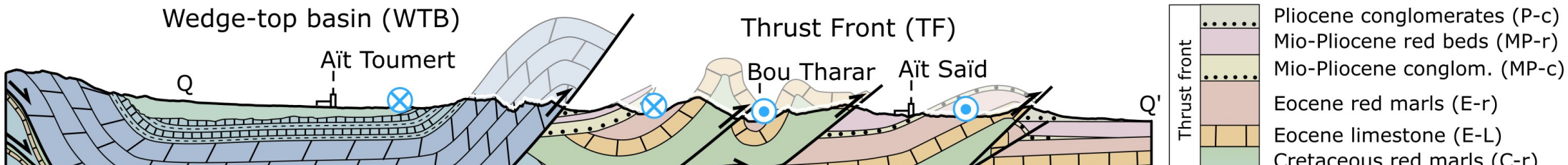
Wedge-top basin (WTB)
Aït Toumert
Q
Thrust Front (TF)
Bou Tharar
Aït Saïd
Q'
Thrust front
Pliocene conglomerates (P-c)
Mio-Pliocene red beds (MP-r)
Mio-Pliocene conglom. (MP-c)
Eocene red marls (E-r)
Eocene limestone (E-L)
Cretaceous red marls (C-r)

Upstream

Wedge-top basin (WTB)

Thrust front (TF)

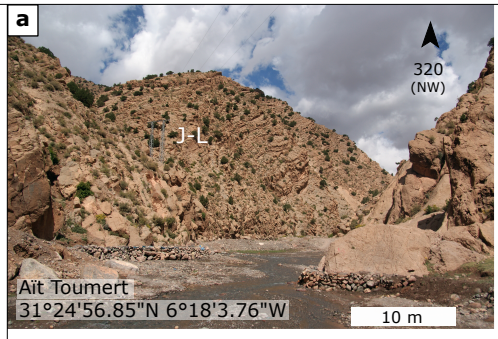

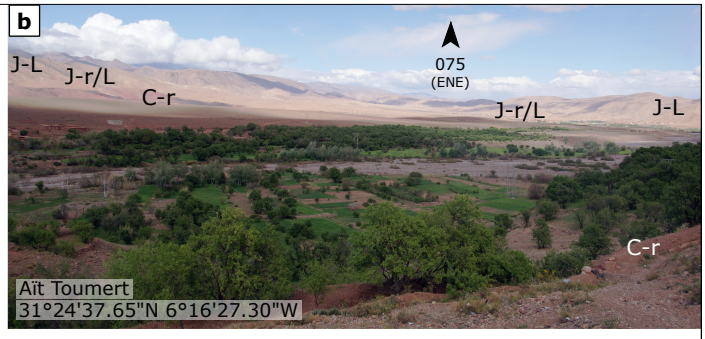

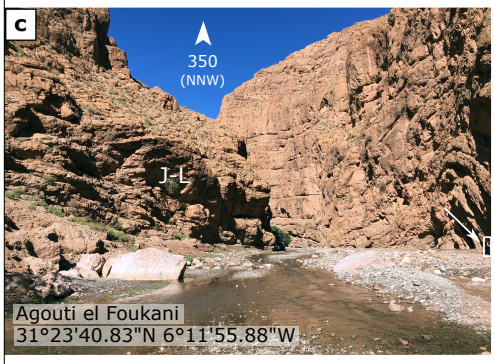

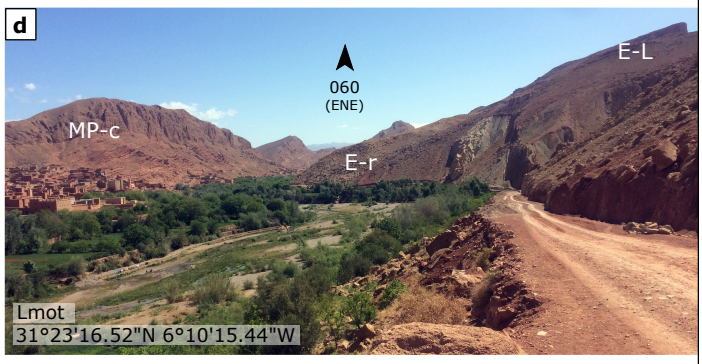

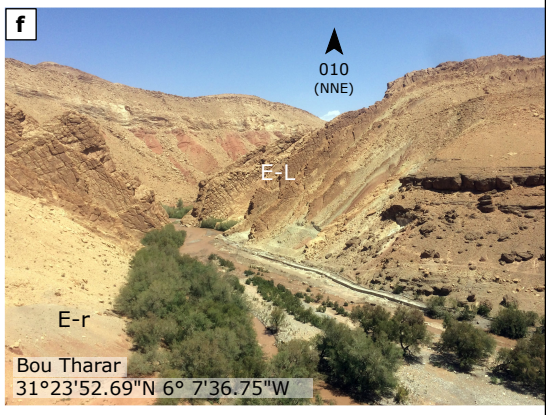

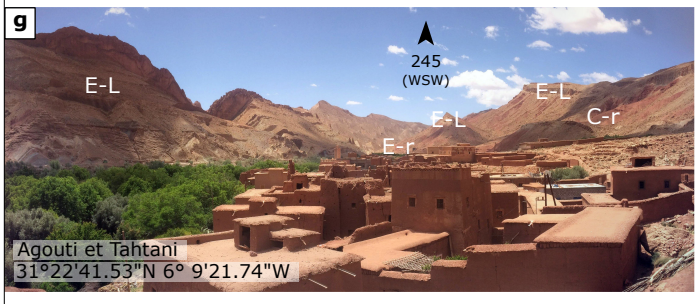

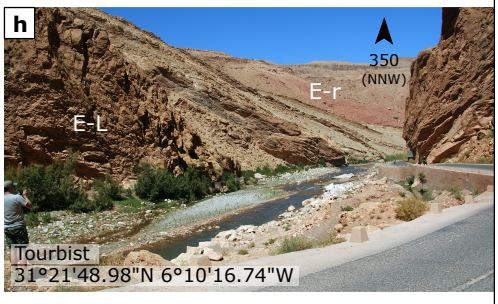

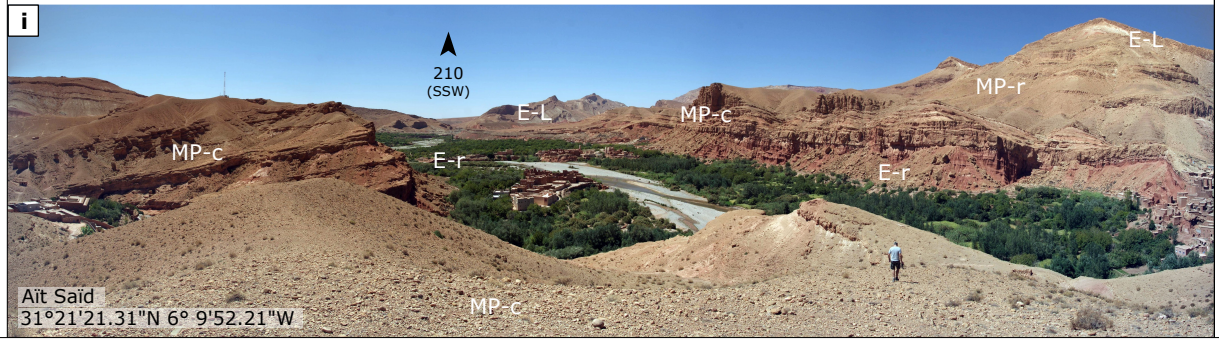

Bou Tharar Valley

Aït Saïd Valley

Downstream

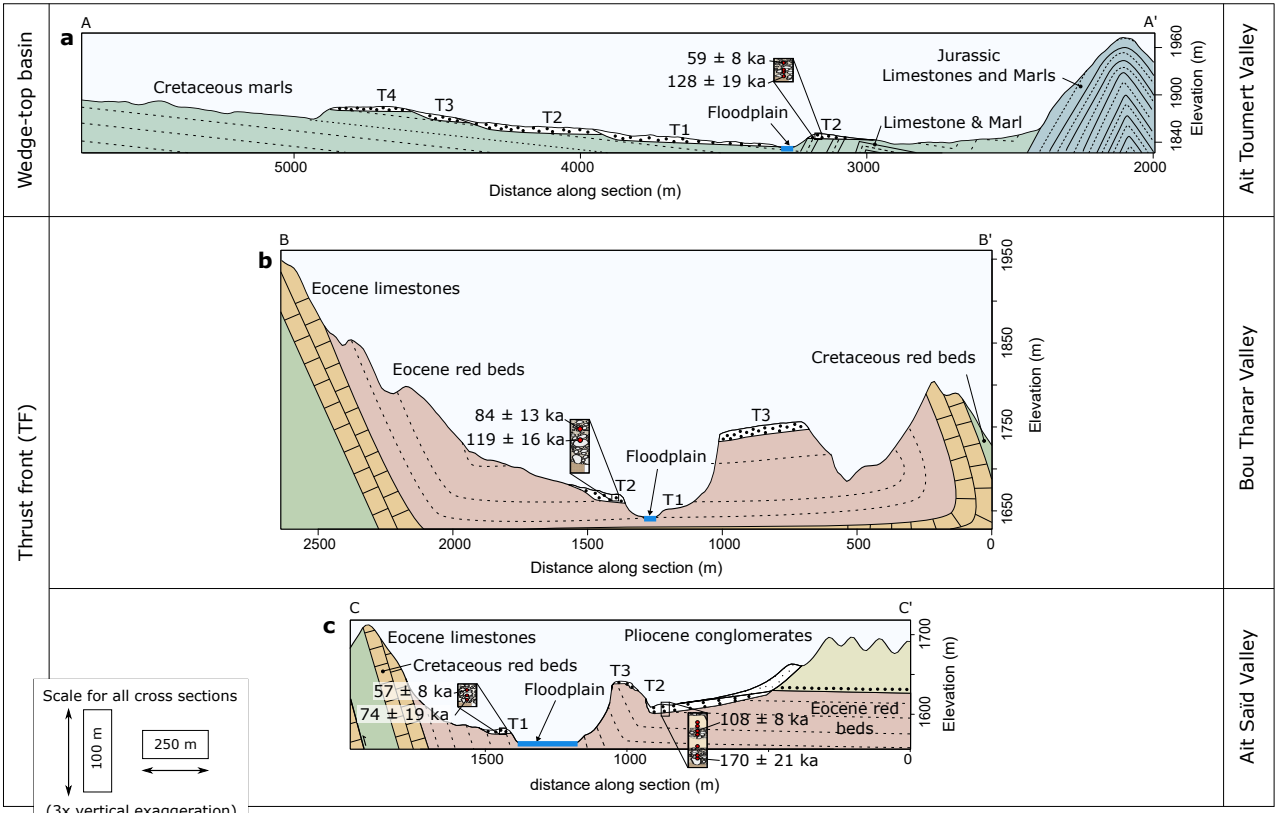
Upstream
Downstream
Wedge-top basin
Thrust front (TF)
Ait Toumert Valley
Bou Tharar Valley
Ait Saïd Valley
a
A
A'
Cretaceous marls
T4
T3
T2
T1
Floodplain
59 ± 8 ka
128 ± 19 ka
Jurassic
Limestones and Marls
Limestone & Marl
Elevation (m)
Distance along section (m)
b
B
B'
Eocene limestones
Eocene red beds
Cretaceous red beds
84 ± 13 ka
119 ± 16 ka
Floodplain
T3
T2
T1
Elevation (m)
Distance along section (m)
c
C
C'
Eocene limestones
Pliocene conglomerates
Cretaceous red beds
57 ± 8 ka
74 ± 19 ka
Floodplain
T3
T2
T1
108 ± 8 ka
Eocene red beds
170 ± 21 ka
Elevation (m)
distance along section (m)
Scale for all cross sections
100 m
250 m
(3x vertical exaggeration)

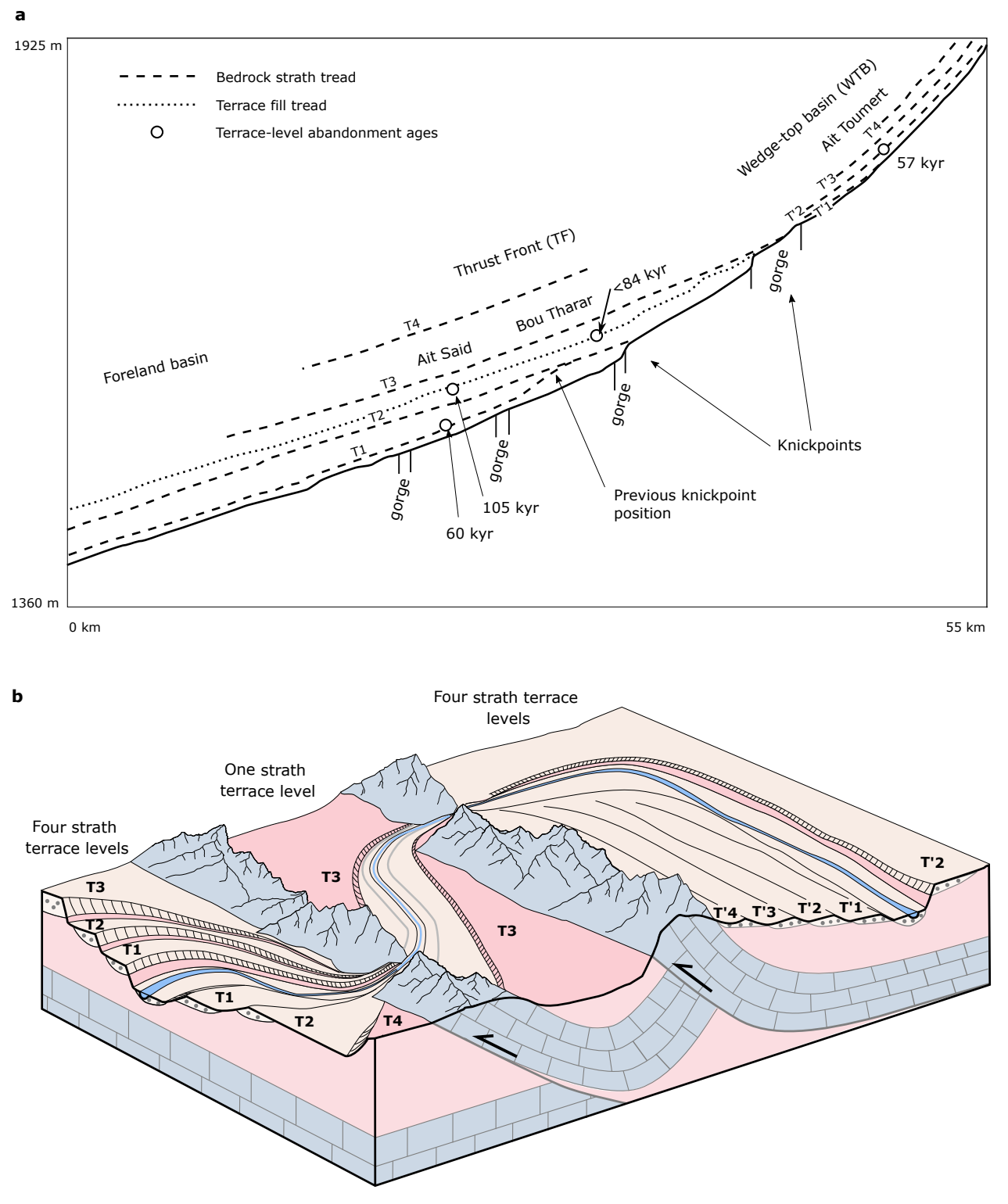
a
1925 m
Bedrock strath tread
Terrace fill tread
Terrace-level abandonment ages
Wedge-top basin (WTB)
Ait Toumert
T'4
T'3
T'2
T'1
57 kyr
Thrust Front (TF)
T4
Bou Tharar
<84 kyr
Foreland basin
Ait Said
T3
T2
T1
gorge
gorge
gorge
gorge
Knickpoints
105 kyr
Previous knickpoint position
60 kyr
1360 m
0 km
55 km
b
Four strath terrace levels
One strath terrace level
Four strath terrace levels
T3
T2
T1
T3
T1
T2
T4
T3
T'4
T'3
T'2
T'1
T'2

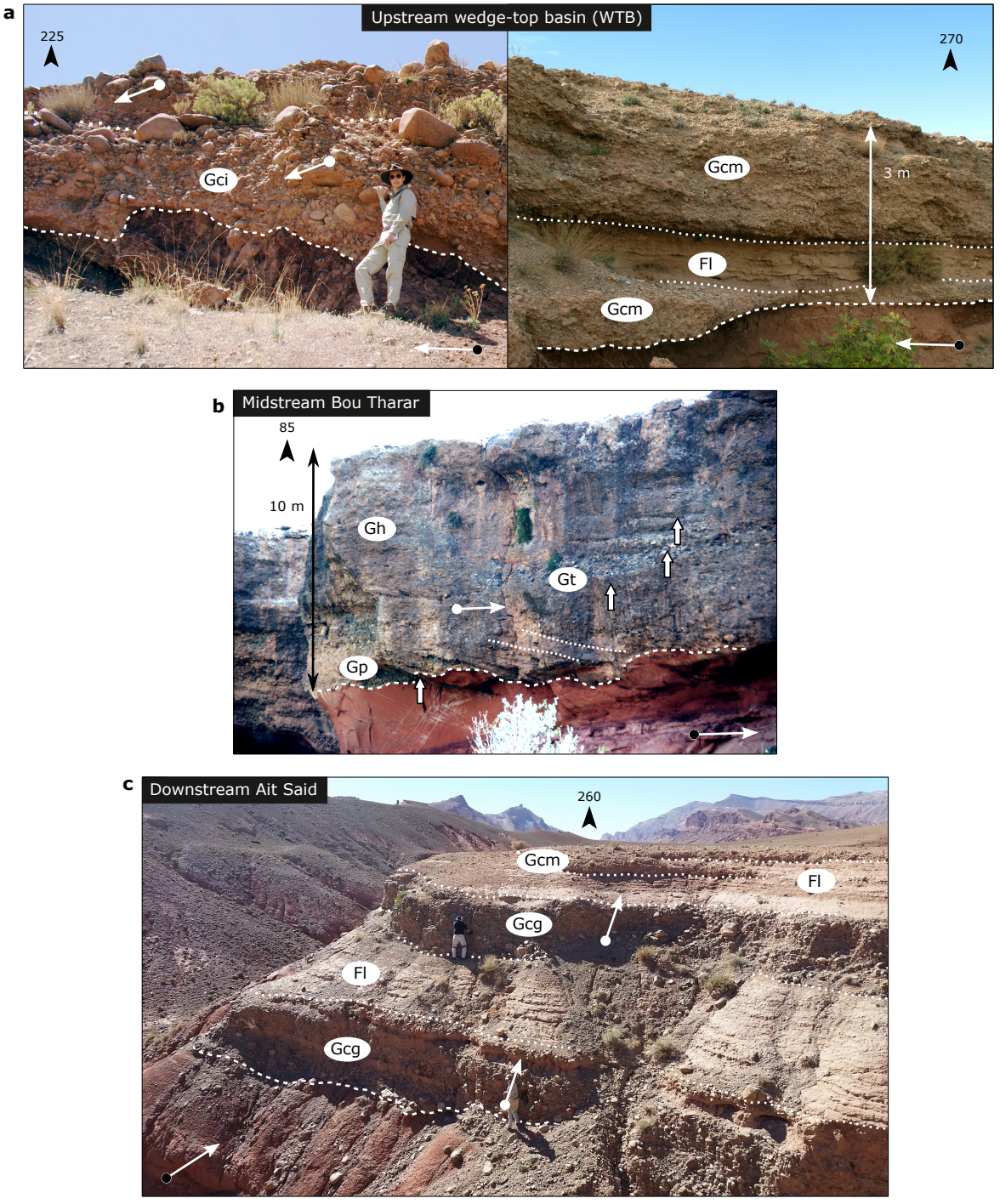
a
Upstream wedge-top basin (WTB)
225
Gci
270
Gcm
3 m
Fl
Gcm
b
Midstream Bou Tharar
85
10 m
Gh
Gt
Gp
c
Downstream Ait Said
260
Gcm
Fl
Gcg
Fl
Gcg

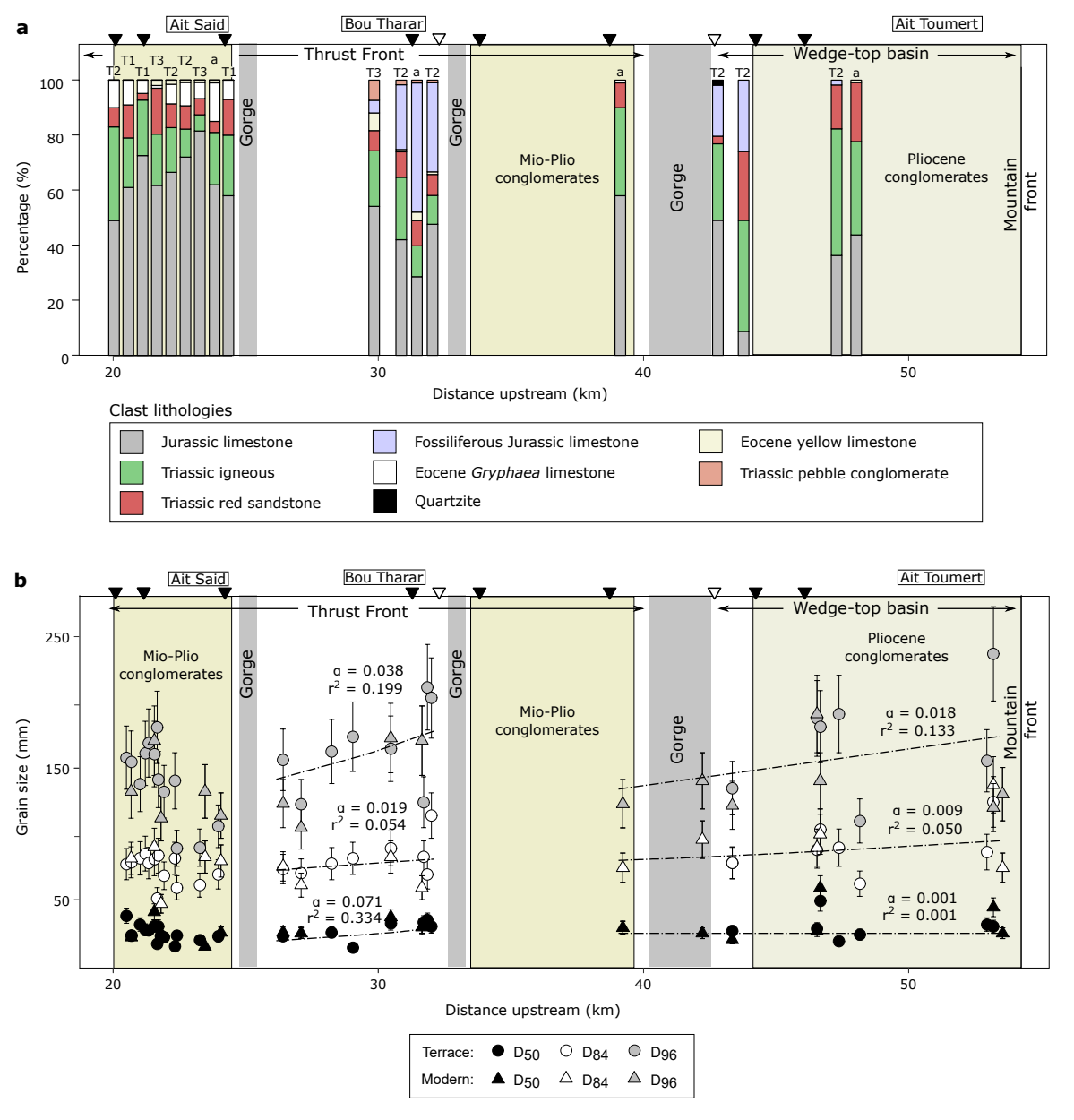
a
Ait Said
Bou Tharar
Ait Toumert
Thrust Front
Wedge-top basin
T2 T1 T1 T3 T2 T2 T3 a T1
T3 T2 a T2
a
T2 T2
T2 a
Gorge
Gorge
Gorge
Mio-Plio conglomerates
Pliocene conglomerates
Mountain front
Percentage (%)
0
20
40
60
80
100
20
30
40
50
Distance upstream (km)
Clast lithologies
Jurassic limestone
Triassic igneous
Triassic red sandstone
Fossiliferous Jurassic limestone
Eocene Gryphaea limestone
Quartzite
Eocene yellow limestone
Triassic pebble conglomerate
b
Ait Said
Bou Tharar
Ait Toumert
Thrust Front
Wedge-top basin
Mio-Plio conglomerates
Pliocene conglomerates
Gorge
Gorge
Gorge
Mio-Plio conglomerates
Mountain front
α = 0.038
r² = 0.199
α = 0.019
r² = 0.054
α = 0.071
r² = 0.334
α = 0.018
r² = 0.133
α = 0.009
r² = 0.050
α = 0.001
r² = 0.001
Grain size (mm)
50
150
250
20
30
40
50
Distance upstream (km)
Terrace: D50 D84 D96
Modern: D50 D84 D96

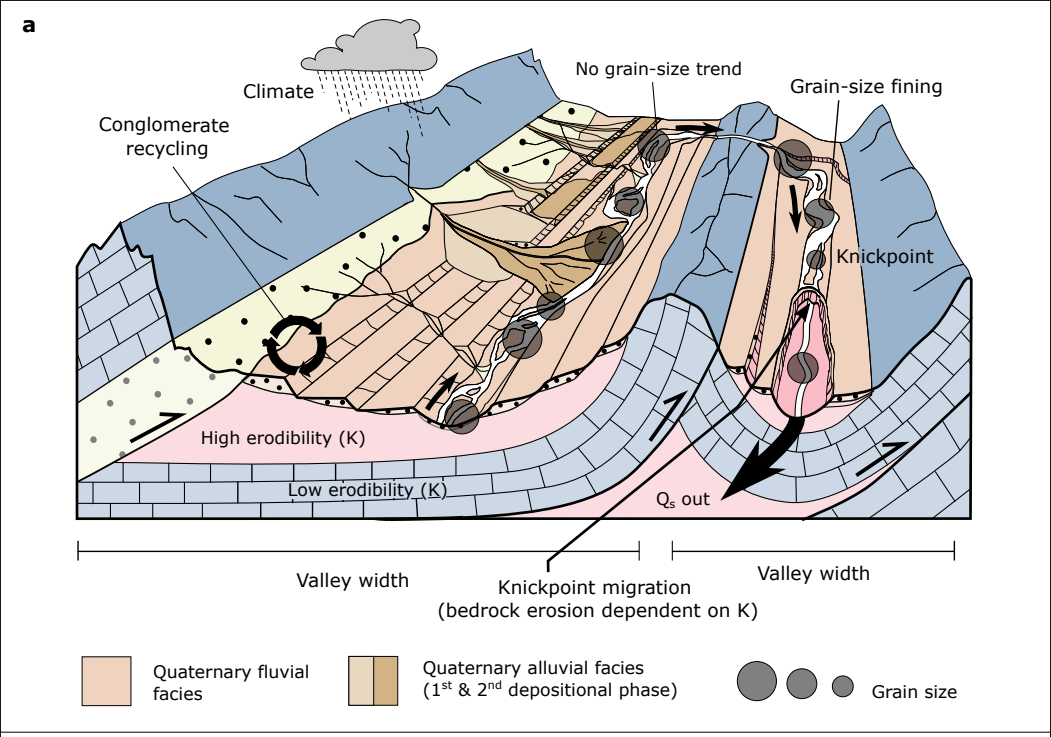
a
Climate
Conglomerate recycling
No grain-size trend
Grain-size fining
Knickpoint
High erodibility (K)
Low erodibility (K)
Q_s out
Valley width
Knickpoint migration (bedrock erosion dependent on K)
Valley width
Quaternary fluvial facies
Quaternary alluvial facies (1st & 2nd depositional phase)
Grain size

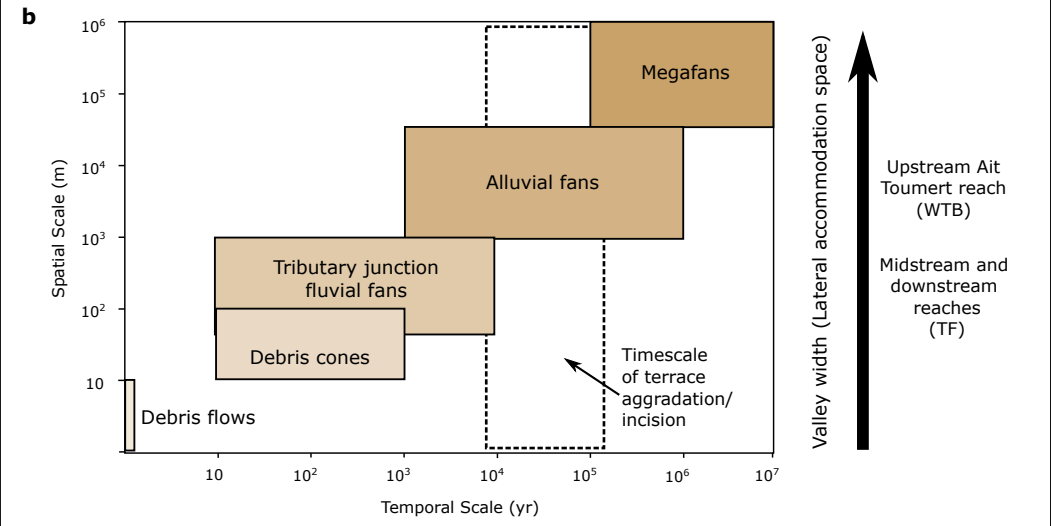
b
Spatial Scale (m)
10^6
10^5
10^4
10^3
10^2
10
Megafans
Alluvial fans
Tributary junction fluvial fans
Debris cones
Debris flows
Timescale of terrace aggradation/ incision
10
10^2
10^3
10^4
10^5
10^6
10^7
Temporal Scale (yr)
Valley width (Lateral accommodation space)
Upstream Ait Toumert reach (WTB)
Midstream and downstream reaches (TF)

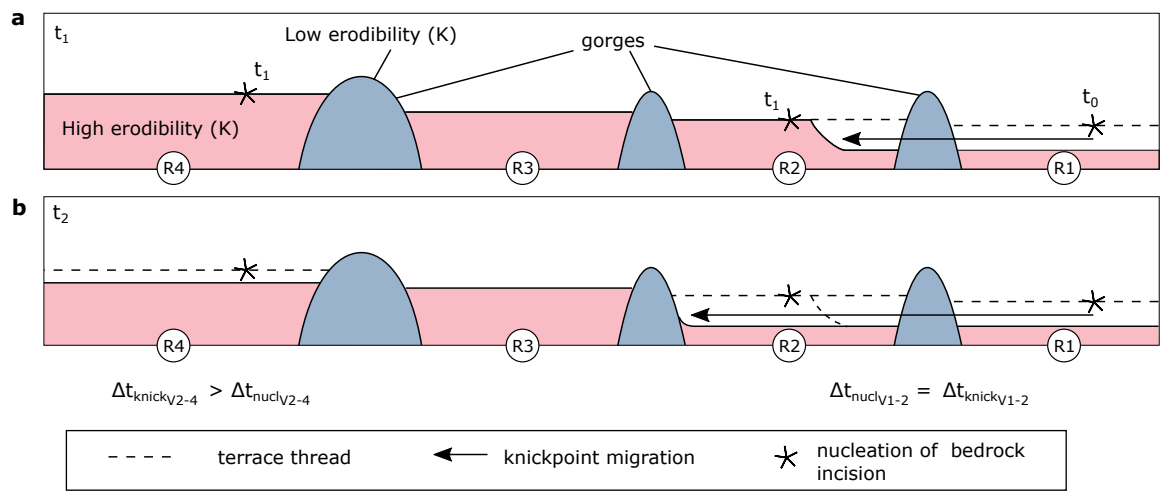
a
t1
Low erodibility (K)
gorges
t1
t1
t0
High erodibility (K)
R4
R3
R2
R1
b
t2
R4
R3
R2
R1
Δtknick V2-4 > Δtnucl V2-4
Δtnucl V1-2 = Δtknick V1-2
terrace thread
knickpoint migration
nucleation of bedrock incision

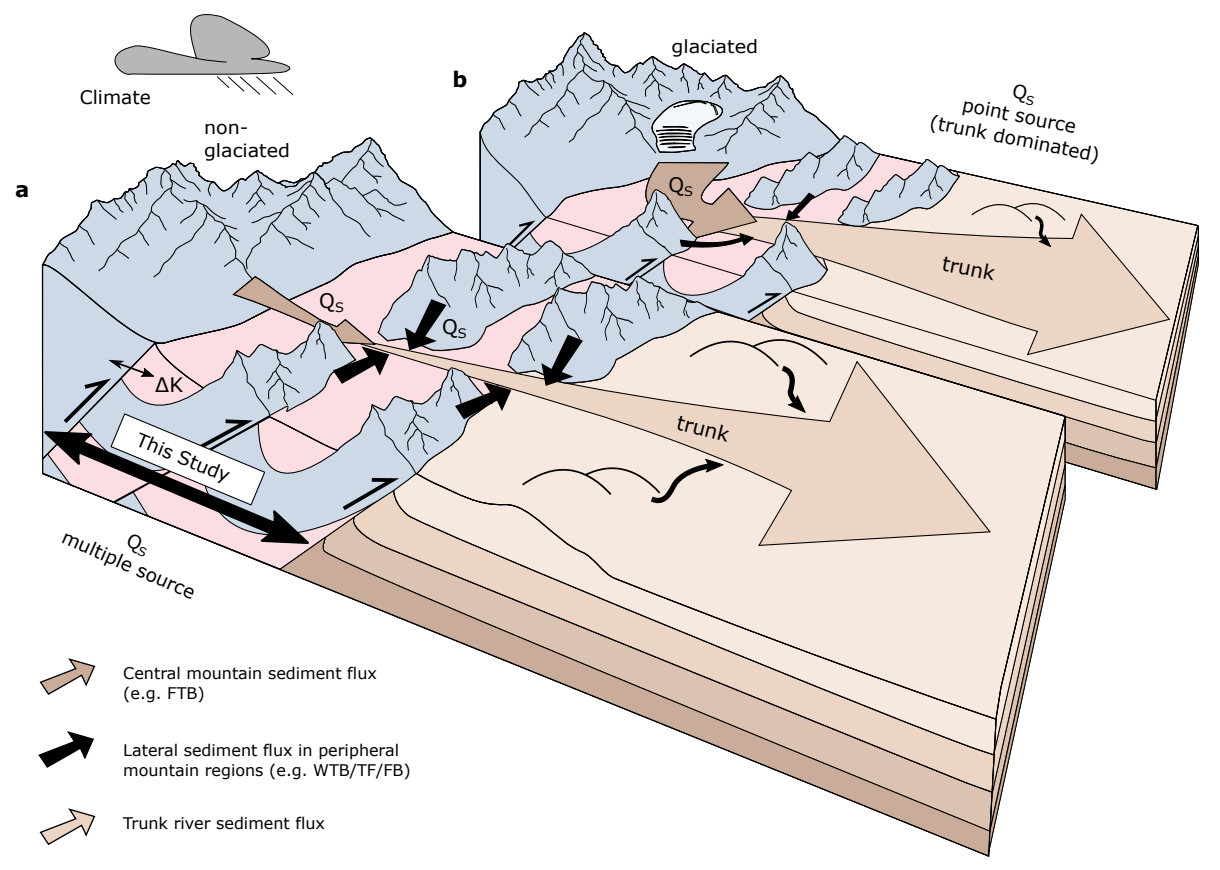
Climate
a
non-
glaciated
b
glaciated
Q_s
point source
(trunk dominated)
Q_s
trunk
Q_s
Q_s
ΔK
This Study
trunk
Q_s
multiple source
Central mountain sediment flux
(e.g. FTB)
Lateral sediment flux in peripheral
mountain regions (e.g. WTB/TF/FB)
Trunk river sediment flux